CHAPTER 8

MATERIAL CIRCULATION THROUGH TIME: CHEMICAL DIFFERENTIATION WITHIN THE MANTLE AND SECULAR VARIATION OF TEMPERATURE AND COMPOSITION OF THE MANTLE

TSUYOSHI KOMIYA

Department of Earth and Planetary Sciences, Tokyo Institute of Technology, Tokyo 152-8551, Japan; E-mail: tkomiya@geo.titech.ac.jp

Abstract

In this chapter, we describe that recent progress of our study of Precambrian geology and geochemistry, and present a synthetic view of the evolution of the solid earth including mantle dynamics and surface geology and environment. The recognition of an accretionary complex and oceanic plate stratigraphy in the 3.8 Ga Isua Supracrustal belt clearly indicates the presence of open sea and the operation of plate tectonics in the early Archean. The change of PT paths of subduction-related metamorphism through time shows that a hotter geothermal gradient at the subduction zone more frequently caused slab melting in the Precambrian, and that the transformation of basaltic crust to a heavy residue after slab melting was a driving force of Precambrian-type plate tectonics. We estimated that the potential mantle temperature of the upper mantle was about 1480°C in the Archean and was hotter by ca. 150–200°C than the modern mantle based on composition of 3.8 to 1.9 Ga MORB-related greenstones. The temperature decreased not monotonously but episodically. The high temperature increased its Rayleigh number by about 30 times, and decreased its viscosity by about one-third, but it complementarily raised the amount of accumulated slab material in the mantle transition zone to trigger off their frequent flushing to the lower mantle. The estimated FeO content of the Archean upper mantle was higher, ca. 10 wt% , and was constant until the early Proterozoic, and then it decreased. Segregation of iron grains from subducted oceanic crust during slab penetration into the lower mantle is a plausible mechanism to decrease the FeO content in the mantle. The growth curve of the continental crust obtained from U-Pb ages of detrital zircons indicates the sudden increase at 2.8–2.7 and 2.0–1.7 Ga. The sudden growth of continents, the worldwide presence of LIPs and many continental collisions at those times imply mantle overturn or extensive exchange between the upper and lower mantle materials, caused by successive upwelling and dowelling of giant superplumes. The mantle overturn events influenced both the surface environment and solid earth. The segregation of iron grains produced ferric iron as a by-product to make the mantle oxidized. In addition, the upwelling of the lower mantle materials through superplumes to the upper mantle increased the $Fe^{3+}/\sum Fe$ in the upper mantle to oxidize it. The change of redox condition of influx gases from reduced to oxidized weakened the suppression by reduced gases against biological oxygenation of the surface environment,

D. A. Yuen et al. (eds.), Superplumes, 187–234.
© 2007 *Springer.*

and consequently the surface environment became oxic in the early Proterozoic after a mantle overturn. Moreover, the formation of large continents before and their break-up after the mantle overturn, produced wide habitats for photosynthetic lives, and helped biological oxidation at the surface.

1 INITIATION OF PLATE TECTONICS AND THE DRIVING FORCE

1.1 Geological evidence for initiation of plate tectonics in the Early Archean

Immediately after the establishment of plate tectonics in the early 1970s, Dewey and Spall (1975) proposed another question: "when did the operation of modern-style plate tectonics began on the Earth?" In those days, there were two opposing schools of thought. First, there was the view that the plate tectonic regime begin at the earliest stage of the evolving earth as suggested by the geochemistry of greenstones (Hart et al., 1970; Condie, 1972, 1982), geophysical considerations (Bickle, 1978; Arndt, 1983; Nisbet and Fowler, 1983) and the geological similarities with Phanerozoic orogenic belts (Burke et al., 1976). The other school suggested that the tectonic regime was typified by vertical movement-dominated orogenies until the late Proterozoic (Wynne-Edwards, 1976; Kröner, 1977, 1981; Piper, 1982). The latter school listed the following features disfavoring the concept of plate tectonics in the Archean: absence of (1) ophiolites, (2) Franciscan-type mélange, and (3) blueschists, all of which characterize divergent or consuming plate boundary processes in the modern Earth. Although an Archean ophiolite was recently reported (Kusky et al., 2001), the counterargument is still raised up (Hamilton, 2003; Stern, 2005). Although geological evidence for plate tectonics and accretion of oceanic crust has been reported in some Archean terrains (Kusky, 1989; Hoffman, 1991; Calvert et al., 1995), definitive criteria are still ambiguous (Bickle et al., 1994; Kusky and Winsky, 1995). Plate tectonics requires two necessary factors; rigidity of lithosphere, and its lateral movement. Komiya and others (1999) proposed criteria for the accretion of oceanic materials to continental lithosphere and the operation of plate tectonics. They comprise the formation of an accretionary complex, oceanic plate stratigraphy in an open sea, evidence for subduction, lateral movement from ridge to trench, and rigidity of an oceanic plate.

The Isua supracrustal belt lies approximately 150 km northeast of Nuuk, Greenland (Fig. 1). It is located in the northeastern part of the Akulleq terrane, which is composed of 3880–3660 Ma Amîtsoq gneiss, and 2820 Ma Ikkattoq gneiss. The former contains enclaves of early Archean supracrustal rocks (Akilia association), whereas the latter contains other enclaves of late Archean supracrustal rocks (Malene supracrustals) and anorthosite complex (McGregor, 1993; Nutman et al., 1996). The Isua belt is, at present, exposed as a fault-bounded tectonic slice, and is in tectonic contact with the tonalitic Amîtsoq orthogneiss on both sides (McGregor, 1973;

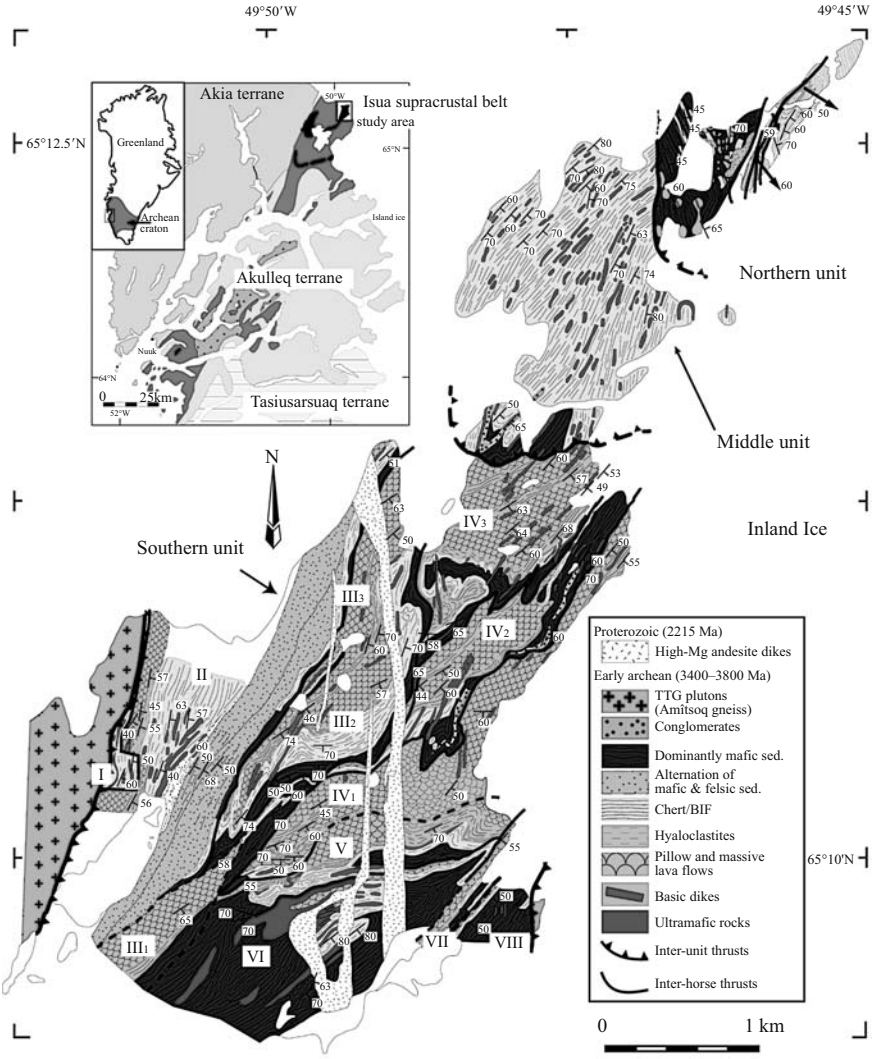


Figure 1. Geologic map of the NE part of the Isua supracrustal belt. The inset is a geotectonic map of southern West Greenland, simplified after McGregor et al. (1991). Three terranes, Akia (gray), Tasiusarsuaq (gray with horizontal bars), and Akulleq are shown. Akulleq terrane is composed of Ikkattoq gneiss (dark gray with white bars), Amîtsoq gneiss (stippled), and supracrustal rocks (black). Post-collision Qôrqut granite (cross) intrudes mainly Akulleq terrane. The Isua supracrustal belt is located in the northeastern corner.



Figure 2. The older basaltic pillow lavas in the Isua supracrustal belt. Some basalts preserve original pillow lava structures in this figure. Each pillow consists of core (gray), mantle (darker gray), rim (white) and matrix (composite from white and dark gray materials).

Bridgwater et al., 1974), but was originally formed as an enclave in the Amîtsoq gneiss. The Isua belt comprises five Early Archean major lithologic units: (1) a mafic-felsic turbidite sequence, including minor interbedded conglomerate, (2) chert and banded iron-formation, (3) pillow lava (Fig. 2), massive lava, pillow breccia, and hyaloclastite, (4) dolerite-gabbro intrusives related to (3), and (5) ultramafic rocks, plus mid-Archean and early Proterozoic intrusions (Fig. 1). The area is subdivided into three units, Northern, Middle, and Southern, by structural breaks defined by low-angle thrusts. The lower half of the Northern Unit is a highly disrupted mélange (Type II, Cowan, 1985), with blocks of greenstone and chert. More than 37 angular to subrounded blocks of greenstone are randomly embedded in a highly sheared muddy matrix, together with several blocks of chert with or without BIF. The upper half is composed of more than four subunits bounded by layer-parallel thrusts. Each subunit is composed of pillow lava or sheet flow greenstone at the bottom, overlain by layered chert/BIF. BIF layers occur at the bottom of the sedimentary sequence, whereas white chert becomes more abundant through the transition of white/blue chert in the upper part. The Middle Unit is mainly composed of dominant NS-trending chert layers, and contains mafic turbidite sequence associated with felsic sandstone, mudstone, calcareous sandy shale, and minor conglomerate near the southern margin.

The Southern Unit displays very clear geological evidence that the Isua supracrustal belt originated from an accretionary complex. It is composed of ultramafic rocks, a basaltic lava flow sequence of massive and pillow lava (Maruyama et al., 1991a) and hyaloclastite, and a sedimentary sequence of pelagic chert and BIF, and terrigenous

turbidite and conglomerate. Cherts and associated sediments form several belts bound by layer-parallel faults, converging in some cases and diverging in others (Fig. 1). Duplex structures are on scales of meters to a few km. At least eight major subunits with horses are defined by the layer-subparallel faults. We reconstructed the original lithostratigraphy within each horse by removing folds and/or thrusts, based on detailed sketches of the outcrops. The reconstructed lithostratigraphies within horses are simple and mutually similar, each consisting of pillow basalt, chert, and turbidite in ascending order (Fig. 3). Major tectonic breaks separating horses on both sides are commonly layer-parallel faults.

The stratigraphic top within each horse always faces southeastward, except in a few strongly folded areas. Petrographic examination of chert indicates that no continental or arc materials occur within the chert beds and underlying pillow lava flows. Detrital materials start to appear in thin laminated chert beds after the end of the major chert deposition, and become common in the turbidite layers. The sequential change of sedimentary lithology, from chert to turbidite, is common to all horses. The

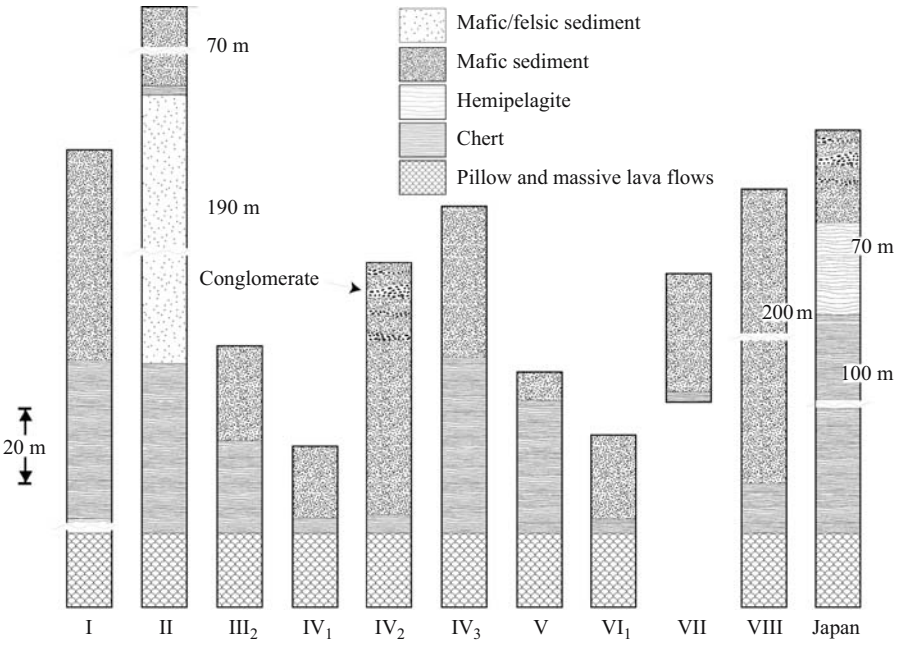


Figure 3. Lithostratigraphies of Duplexes I to VIII. Each lithostratigraphic unit is composed of metabasite, chert, muddy chert and mafic sediment, in ascending order. The metabasite consists of a pile of pillowed basalts with massive basaltic flows and hyaloclastites. A reworked hyaloclastite with rough surfaces and numerous metamorphic garnet megaporphyroblasts occurs at the top. Mafic sediment with graded bedding covers the chert at the top. Muddy chert occurs as a transitional sediment between the chert and the mafic sediment. The reconstructed lithologies are comparable to the Phanerozoic oceanic plate stratigraphy in Japan.

reconstructed lithostratigraphy is remarkably similar to oceanic plate stratigraphy of circum-Pacific accretionary complexes (Isozaki et al., 1990; Matsuda and Isozaki, 1991; Wakita and Metcalfe, 2005). The presence of duplexes indicates the geological structure was formed by layer-parallel shortening, whereas evidence of oceanic plate stratigraphy means lateral movement from pelagic ridge to continental margin. The lines of evidence indicate that the Isua supracrustal belt is the oldest accretionary complex. Komiya and others (1999) demonstrated that in the Southern Unit, and possibly in the whole Isua supracrustal belt, an accretionary complex formed through accretion of oceanic crust to the hangingwall, by duplexing. A sequence of duplexing scenarios can be reconstructed as follows. The structural bottom is Duplex I, and the top is Duplex VIII, as judged by the southward polarity of duplexing. The younger horses develop downward; therefore, the oldest duplex is VIII. Accretion proceeded from Duplex VIII to I with time. Within a given Duplex, the southeastern horse is the oldest. The similar lithostratigraphy within each horse suggests that the oceanic crust segments subducted in the same area and period. The mode of formation of the duplex structure throws light on the direction of the growth of the accretionary prism and the subduction of oceanic lithosphere. The duplex polarity is defined by the direction of convergence of faults, which divide horses, and coincides with plate convergence. The southward convergent morphology of the duplex structure is widespread over the mapped area, indicating that the Isua accretionary prism grew from south to north. A paleogeographic reconstruction is shown in Figure 4 to illustrate the sequential events of the accretionary prisms in the Southern Unit at about 3700–3800 Ma (Komiya et al., 1999). Geologic records preserved within turbidite sediments also provide strong constraints on the type of active plate margin. If they were formed along a large continental margin, they would be dominantly quartzofeldspathic. If they

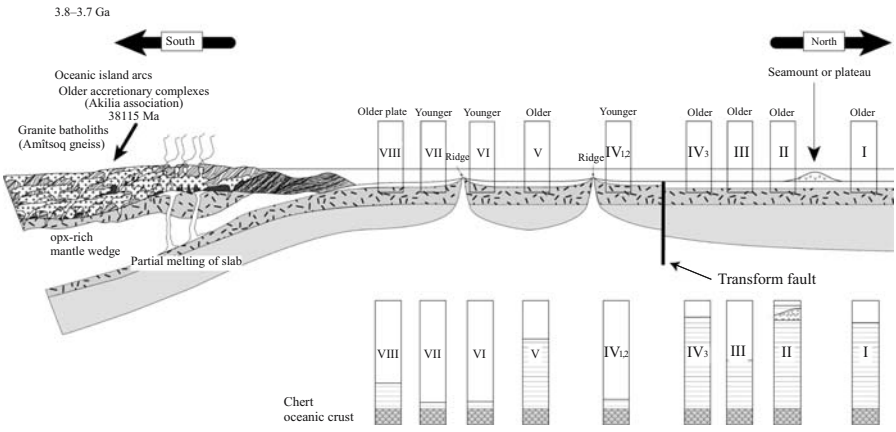


Figure 4. Travel history of Early Archean oceanic lithosphere in the Isua accretionary belt, West Greenland. This diagram shows paleogeographic reconstruction of accreted oceanic lithosphere, followed by successive underthrusting of oceanic crust to form duplexes from Duplex VIII to I with time.

were formed in intra-oceanic environments, such as the present-day western Pacific domains, they would be dominantly mafic in composition. The sedimentary petrology of the turbidite sequences clearly indicates that the Isua accretionary complex was formed in the latter environment, because mafic sediments are dominant in the turbidite sequences. In the Archean, most orogenic belts were formed in intra-oceanic island arcs, and then grew progressively through the collision-amalgamation process.

Evidence of accretion of oceanic materials at subduction zone indicates successive underthrusting of oceanic crust. This suggests that a kind of tectonics similar to the Phanerozoic plate tectonics operated in the Early Archean, but it does not necessarily prove that modern-style plate tectonics were in operation in a strict sense. Evidence of the operation of modern-style plate tectonics on Earth includes: (i) rigid plates, (ii) significant lateral movement of the plate, (iii) multiple plates surrounded by plate boundaries, and (iv) linearity of plate boundaries. However, evidence of (i) and (ii) are necessary and sufficient to identify the existence of modern-style plate tectonics, because horizontal passive movement of rigid plates results in the presence of multiple plates (iii) and in linearity of plate boundaries (iv) (Oldenburg and Brune, 1972; Turcotte and Schubert, 1982). In other words, the rigidity of an oceanic plate is also necessary to discern whether modern-style plate tectonics or a hybrid of plume and plate tectonics operated (Head and Crumpler, 1990). A comparison with tectonics on Venus provides some perspective because Archean tectonics on Earth has been widely regarded as similar to modern Venusian tectonics. Pillowed basalt at the bottom of the oceanic plate stratigraphy preserved in the Isua supracrustal belt indicates that sea water was present and that open sea extended far from any oceanic island arc. Numerical simulations of temperature and composition of ocean and atmosphere demonstrated that formation of a proto-ocean decreases atmospheric pressure to ca. 10 atm and the surface temperature to ca. 20°C (Tajika and Matsui, 1990). These relations support the idea that the surface temperature was cooled down to less than 100°C in the Early Archean. Knowledge of the composition and thickness of oceanic crust, and the temperatures of the mantle and Earth's surface allows us to reconstruct the structure of an oceanic plate (Fig. 5). Geotherms of oceanic lithosphere as a function of age were calculated based on a model of transient half-space cooling (Turcotte and Schubert, 1982) at given parameters of temperature of the mantle and surface, 1450 and 100°C, 1330 and 0°C and 1450 and 470°C for the early Archean and present Earth and Venus, respectively. In addition, transitions of ductile/brittle deformations of peridotite and diabase are calculated as a function of temperature and pressure for a given steady-state strain rate of a representative tectonic strain rate, 10^{-14} s^{-1} (after Hoffman and Ranalli, 1988). The rheological structure of oceanic lithosphere as a function of age were estimated from oceanic geotherms and the ductile/brittle transitions (Fig. 5 b–d), and indicate that an oceanic plate older than 20 m.y. behaves rigidly even in the Early Archean (Fig. 5c right). The evidence suggests that oceanic plates in the Early Archean were rigid, in contrast to the substantial ductile surface of Venus (Fig. 5d). In summary, there is evidence for (i) rigid plates, (ii) significant lateral movements and (iii) subduction of plates in the Early Archean Isua accretionary complex. The evidence proves that modern-style plate tectonics has been in operation

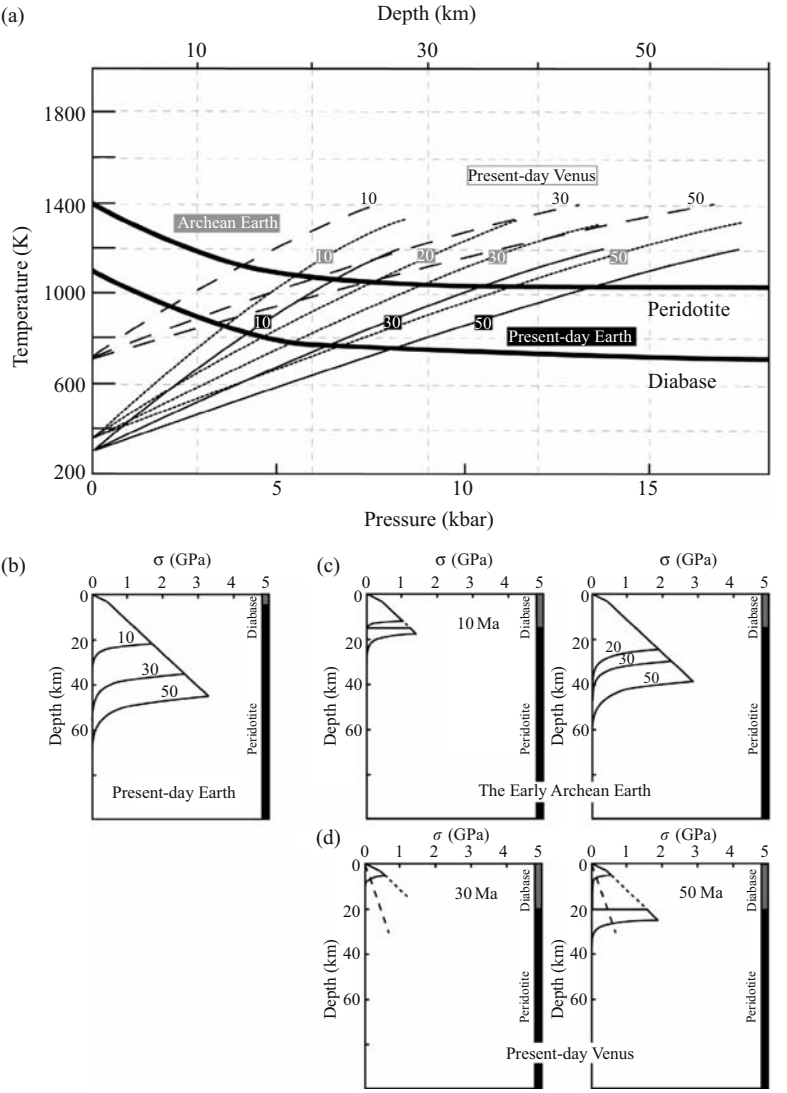


Figure 5. (a) Geothermal gradients of oceanic lithosphere for Earth and Venus at present and in the Archean. The transitions of ductile/brittle behaviour of peridotite and diabase (thick lines) were calculated as a function of temperature and pressure for a given steady-state strain rate of a representative tectonic strain rate, 10^{-14} s^{-1}. Oceanic geotherms for different lithosphere ages given in units of millions of years on the plots are calculated based on a model of transient half-space cooling (Hoffman and Ranalli, 1988). Note that the surface temperature on Venus is 470°C higher than on Earth. (b) Strength profiles in compression for modern oceanic lithosphere as a function of age are given in units of millions of years on the plots. The 7-km thick oceanic crust is modeled as diabase, and the upper mantle as peridotite. (c) Strength profiles in compression are for Archean oceanic lithosphere, 10 m.y. old (left) and 20–50 m.y. old (right). A 15-km thick crust is modeled. (d) Strength profiles in compression for Venusian oceanic lithosphere, 30 m.y. old (left) and 50 m.y. old (right). A 20-km thick crust is modeled (Buck, 1992).

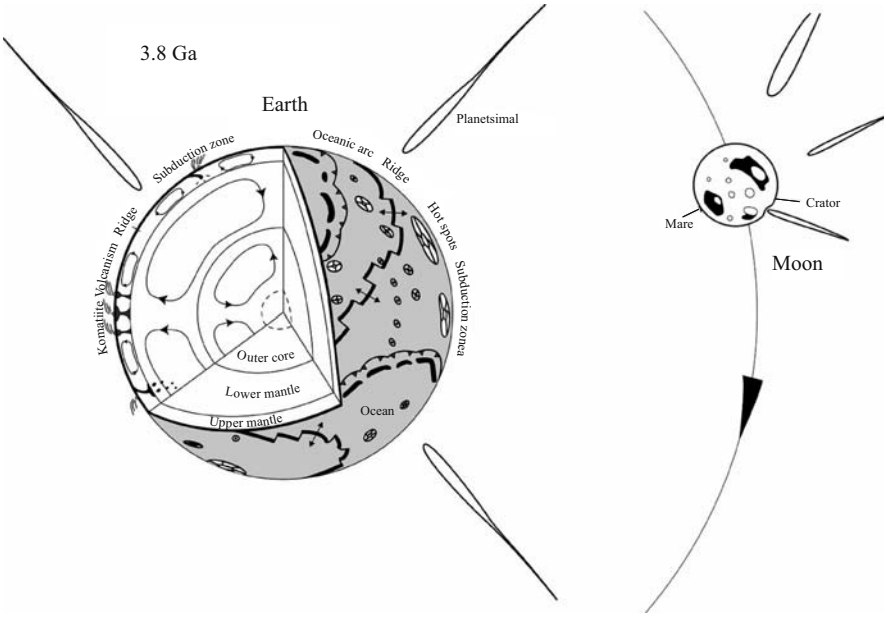


Figure 6. A speculative cartoon showing 3.8 Ga planet Earth and its satellite Moon. Plate tectonics had already started but there was no solid inner core. Double-layered mantle convection with episodic leakage between the upper and lower mantle boundary was predominant. There were no large continents and a number of intra-oceanic island arcs, and abundant off-ridge volcanism related to mantle upwellings. The satellite, Moon, was active only by heavy extra-terrestrial bombardments and related Mare volcanism.

since the Early Archean, and quite different from the Earth's satellite, Moon, which was resurfaced by heavy extraterrestrial bombardment and by related Mare volcanism (Fig. 6).

1.2 Precambrian-type and Phanerozoic-type plate tectonics and the driving force of Precambrian-type plate tectonics

Application of accretionary geology concepts to Archean greenstone belts has revealed that modern-style plate tectonics were already in operation in the Early Archean. However, geophysical calculations of the relationship between the temperature of the mantle and the density of an oceanic plate contradict the geological evidence for the operation of plate tectonics in the Early Archean, because an Archean thin (∼40 km) oceanic plate capped by a thick (∼20 km) oceanic crust may have been lighter than the asthenospheric mantle (Davies, 1992). In the Phanerozoic, oceanic lithosphere is heavier than asthenosphere because of a negligibly thin oceanic crust (Kono and Yoshii, 1975). Therefore, even if the basaltic crust does not transform into eclogite during subduction, the oceanic lithosphere can subduct into the mantle

due to its negative buoyancy. However, in the Archean, Davies (1992) suggested that oceanic lithosphere could not subduct directly into the asthenosphere because it was lighter than the asthenosphere. Therefore, Another driving force would be required for subduction of the oceanic lithosphere into the mantle in the Archean.

Grambling (1981) postulated a secular variation of metamorphic facies series from a compilation of Archean metamorphic data. However, determination of the tectonic setting of metamorphism is essential for investigation of secular change, because the metamorphic facies series strongly depends on the tectonic setting of the metamorphism (Miyashiro, 1973). Recently, the secular change of PT paths of a subducted slab was estimated from a petrological study of the oldest progressive regional metamorphism of the Isua supracrustal belt (Hayashi et al., 2000; Komiya et al., 2002a) and from a compilation of subduction-related metamorphisms (Maruyama et al., 1996; Hayashi et al., 2000). This work was based on a mineralogical and petrological study of metabasites and metapelites affected by Archean progressive metamorphism from the Isua belt, West Greenland, and it proposed a driving force for Archean plate tectonics.

The area of the Isua supracrustal belt is divided into four metamorphic zones based on mineral assemblages and microprobe analyses of coexisting minerals in metabasites and metapelites. Especially we selected mineral assemblages in moderately magnesian metabasites, where chlorite is 50–60 in $Mg^{\#}$ (Fig. 7a), because

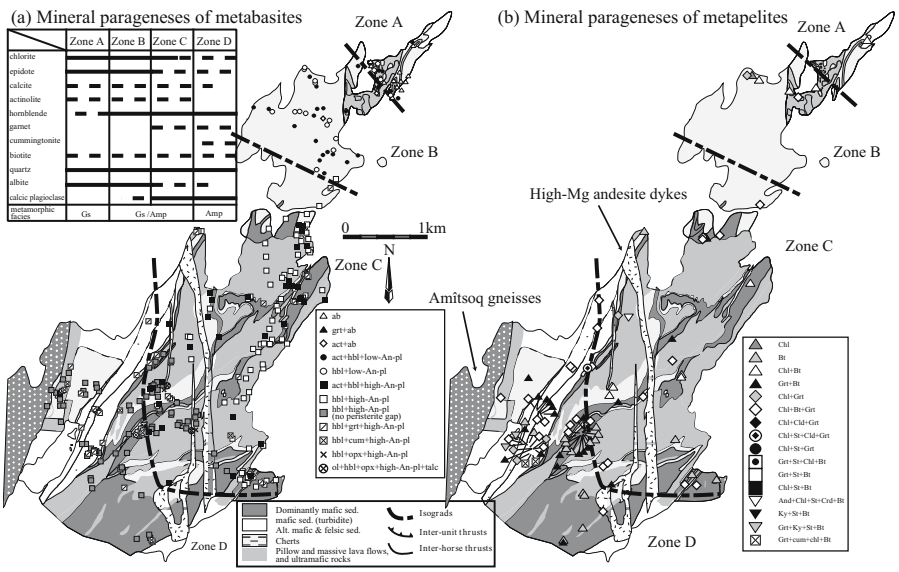


Figure 7. Mineral assemblages of metabasites (a) and metapelites (b) in the northeastern area, which are subdivided into four zones based on mineral assemblages and the anorthite content of plagioclase in metabasite. The metamorphic grade ranges from greenschist facies in the northernmost area through epidote-amphibolite transition to amphibolite facies in the southern Unit.

the composition of calcic amphiboles strongly depends on the whole rock composition (Hayashi et al., 2000). Zone A is defined by the Gs-facies mineral assemblage, Chl + Ep + Ab + Qz, and Zone B by the appearance of Ca-amphiboles, either Act and/or Hbl, together with Ab and/or oligoclase; the mineral assemblage is Chl + Ep + two Ca-amphiboles + peristeritic Pl + Qz, that shows the transition between Gs and Amp facies. Zone C is defined by the appearance of calcic plagioclase, the appearance of a single amphibole of hornblende composition in magnesian samples, and the appearance of Grt coexisting with Hbl in iron-rich samples. The diagnostic mineral assemblage in metabasites is Chl + Ep ± Act + Hbl + Pl + Qz. Zone D is defined by disappearance of two Ca-amphiboles-bearing samples, concomitant with a high anorthite (An) content of plagioclase and a single Ca-amphibole of hornblende composition in moderately magnesian samples; the mineral assemblage is Chl + Ep + Hbl + calcic Pl + Qz. High magnesian rocks contain two amphiboles, cummingtonite (Cum) and Hbl.

About 120 samples have mineral assemblages of typical pelitic systems, and most have mineral assemblages of either Chl + Bt or Grt + Bt, together with Ms and Qz. However, some samples have diagnostic mineral assemblages that enable estimates of metamorphic temperatures and pressures (Komiya et al., 2002a). In Zone A Grt is absent and Chl and Bt are present together with phengite (Phn) and Qz. Grt becomes stable in the northeastern side of Zone B. The mineral parageneses of Chl + Grt or Chl + Bt + Grt are found in some metapelitic rocks, indicating the stable coexistence of Grt and Chl. In Zone C Cld and St occur in aluminous samples together with Grt, Chl, Qz, and Phn. Although the mineral assemblage of other Zone C rocks is the same as that in Zone B, Fe/(Fe + Mg) ratios of the coexisting minerals are much higher than those in Zone B. In Zone D there are two types of mineral paragenesis: most samples contain the same mineral assemblage of Grt + Chl + Bt as in Zone C, but the distinctive parageneses of Ky + St + Bt, Ky + Chl + Bt or St + Grt + Bt and Ky + Grt + Bt or Ky + Chl + Bt occur on the southern side of the Zone (Fig. 7b). In summary, five reactions are expected in the phase diagram of the KFMAS + MnO system (Symmes and Ferry, 1992; Spear, 1993), Chl1 = Grt + Chl2 (ca. 440°C), Chl + Grt + Ky = Cld (ca. 530°C), Cld = St + Grt + Chl + H_2O (ca. 560°C), Grt + Chl = St + Bt + H_2O (ca. 610°C), and St + Chl = Ky + Bt + H_2O (ca. 620°C) (Komiya et al., 2002a). The PT path of the metamorphism was estimated to be in the intermediate-P/T type metamorphic facies series (Fig. 8). The metamorphism is subduction-related, and was caused by late Archean collision-amalgamation of the Akia and Akulleq terranes (e.g., McGregor et al., 1991), or early Archean subduction of oceanic lithosphere. All Archean metamorphic terrains worldwide belong to the intermediate- or low-P/T type metamorphic series (Fig. 8).

The age of a subducting plate has a significant control on the geotherm (e.g., Defant and Drummond, 1990; Peacock, 1996). Comparison of P-T estimates of Archean metamorphism with Phanerozoic subduction metamorphism indicates that the geothermal gradient of Archean subduction zones was over 200°C higher than in the Phanerozoic (Fig. 8). The Phanerozoic geotherm ranges from low to high P/T-type, depending on the age of the subducted slab, but the Archean geotherm does not

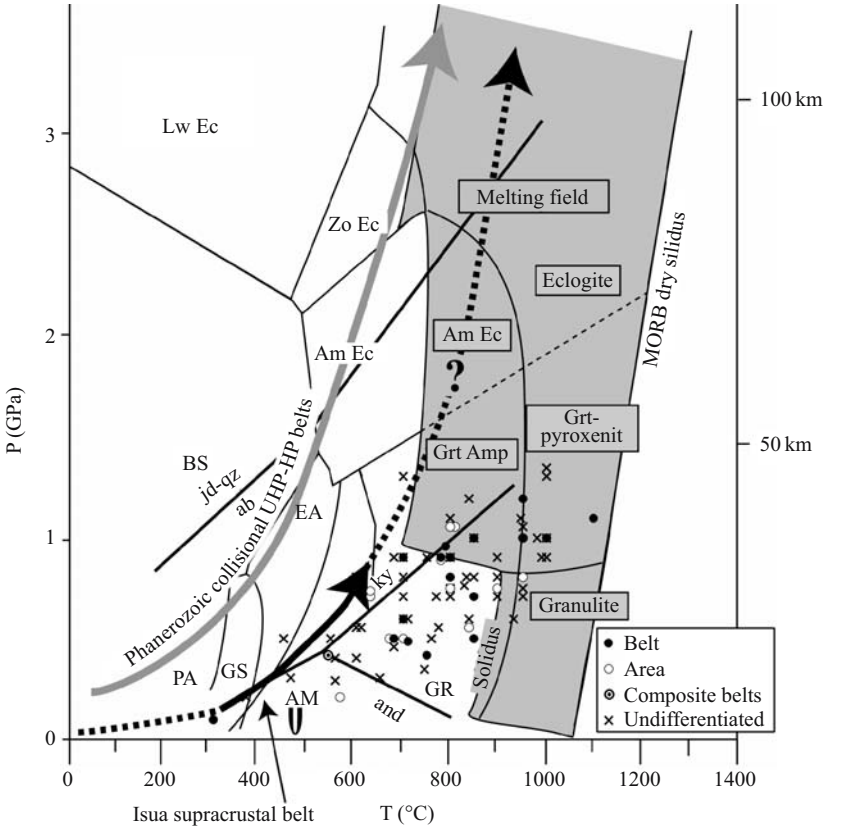


Figure 8. Phase relations of hydrated MORB, modified after Okamoto and Maruyama (1999), and the residual mineral assemblage (shaded region) after partial melting of hydrous Archean basalt (Rapp and Watson, 1995; Vielzeuf and Schmidt, 2001). Also shown are geothermal gradients of Phanerozoic collisional UHP-HP metamorphic belts (Maruyama et al., 1996) and Archean subduction zone metamorphism of the Isua supracrustal belt, accompanied by a recent compilation of P-T estimates of Archean metamorphic belts (Hayashi et al., 2000). Hayashi and others (2000) classified 111 Archean metamorphic terranes into belt, area and composite belts, dependent on the shape. Many Archean metamorphic terrains cannot be simply classified as either "belt" or "area". Among 111 Archean terrains, they identified 20 metamorphic "belts" and 18 "metamorphic areas". The rest of them remain unclassified.

extend to the high P/T side, ranging from low to intermediate P/T-type (Fig. 8). The following three candidates can be considered as a heat source for subduction zone metamorphism with a high geothermal gradient; (1) the overlying mantle wedge and continental crust, (2) the mantle below the oceanic lithosphere and (3) the remaining heat of MORB-formation within the lithosphere. We have calculated the thermal structure of oceanic lithosphere, in order to verify whether the remaining heat of MORB formation within the lithosphere is possible as a heat source for Archean

subduction metamorphism with a high geothermal gradient. The minimum temperature at the base of subducting oceanic crust can be calculated, based on the transient half-space cooling model and diffusivity of 1 $mm^2\ s^{-1}$. In the Phanerozoic, the temperature at the base of a 7-km thick oceanic crust falls below the solidus temperature of hydrated basalt only in 3-m.y after formation at given temperatures of the mantle (1330°C). However, in the case of Archean oceanic lithosphere with a 20 km thick oceanic crust, the temperature at the base of that crust is still higher than the wet solidus even after 15 m.y. at given temperatures of the mantle (1450°C). This calculation indicates that the remaining heat of MORB formation within the lithosphere is a probable heat source for Archean metamorphism with a high geotherm, and even for slab melting.

Although the Isua metamorphism did not reach melting conditions, the simple extension of the P-T path to the higher grades into the melting field in Figure 8 indicates that the hydrated oceanic crust would have been partially melted to produce granitic magma (the protolith of Amîtsoq gneiss). Namely, in the Archean, when the thickness of continental and older oceanic lithosphere combined exceeded ca. 30 km, the high geothermal gradient at the subduction zone led to melting of hydrated oceanic crust to form the tonalite-trondhjemite-granodiorite suite (TTG) (Martin, 1986; Defant and Drummond, 1990) and a denser garnet-bearing residue, such as high-pressure granulite (HGR) and garnet-clinopyroxenite. The calculated densities of basaltic crust, garnet-clinopyroxenite, HGR, and lithospheric and ambient mantle are shown in Figure 9a. The calculation indicates that the average density of lithosphere increases from 3.22 to 3.46 for the oceanic lithosphere with garnet-clinopyroxenite or 3.42 for HGR after slab melting, and that the slab can subduct to mantle depth by the increase of slab-pull force due to TTG melt extraction (Fig. 9a). The calculation suggests that the transformation of basaltic crust to garnet-clinopyroxenite or HGR was a driving force for Archean plate tectonics. There are some differences between plate tectonics in the Archean and at present (Fig. 9). They are (1) thickness of oceanic lithosphere, (2) thickness of the accompanied oceanic crust, (3) average life span of oceanic lithosphere, and (4) the cause of slab-pull (Komiya et al., 2002a). In the Phanerozoic, slab-pull is effective immediately after the birth of oceanic lithosphere, whereas in the Archean slab-pull was achievable only after slab melting. A ratio of the oceanic crust over thickness of the lithosphere of ca. 0.75 is the critical number determining whether slab-pull is effective even just after the birth at a ridge. Geophysical calculation of mantle temperature suggests that the ratio attained the critical value at ca. 1 Ga (Davies, 1992). In addition, compilation of modern and ancient ophiolites also supports the idea that thickness of oceanic crust decreased from ca. 12 to 5 km around 1 Ga (Moores, 1993). This evidence possibly indicates that Phanerozoic-type oceanic lithosphere with a slab-pull force from its birth began to be formed at ca. 1 Ga. In addition, blueschists did not form over the world before the late Proterozoic (Maruyama et al., 1996). The presence of blueschists indicates that the geothermal gradient decreased at subduction zones, and that old oceanic plates began to subduct at that time. This line of evidence and reasoning suggests that plate tectonics switched from a first-stage

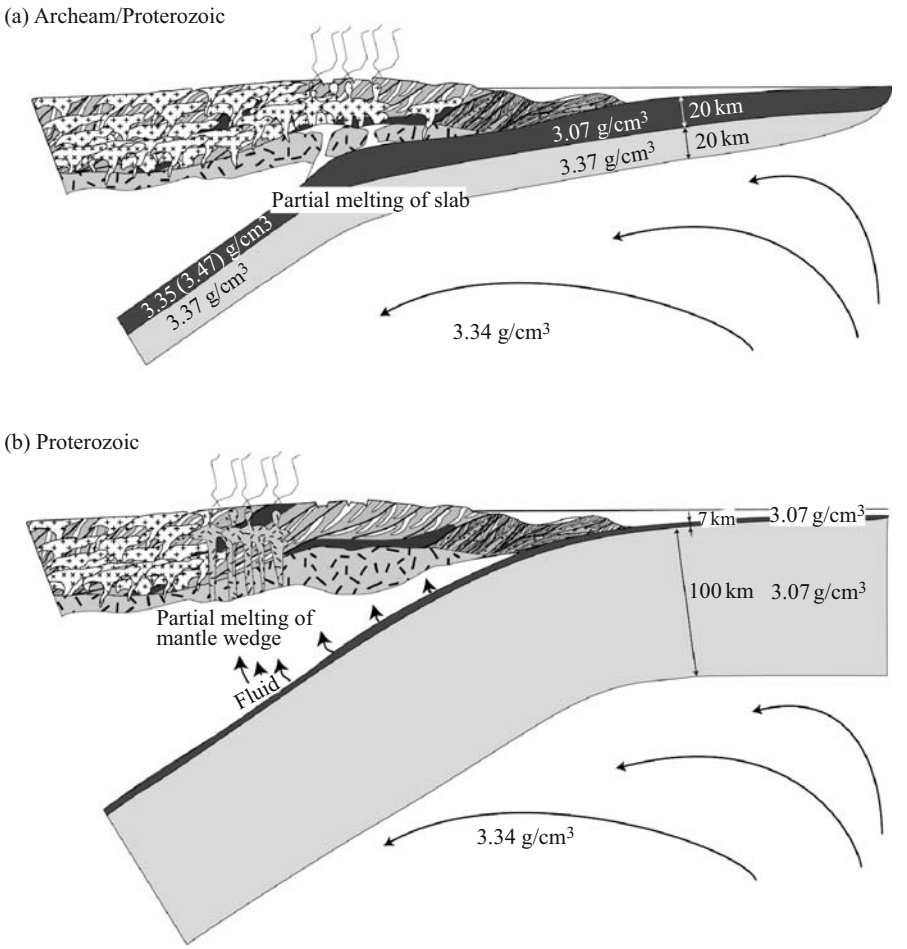


Figure 9. Schematic illustration of subduction zones, showing contrasting tectonic modes of subducting lithosphere. (a) Low-angle subduction of young oceanic lithosphere results in slab melting, supplying felsic magma through the very small volume of mantle wedge to the continent (Precambrian-type). Calculated density profile of Archean oceanic lithosphere indicates formation of highly dense garnet-bearing residues after TTG melt extraction become the slab-pull force. (b) Angle of subduction depends on age of oceanic plate. High-angle subduction of old oceanic lithosphere supplies dehydration fluids to the hanging wall of the mantle wedge (Phanerozoic-type).

with slab melting (Precambrian-type) to a second-stage with/without slab melting (the Phanerozoic-type) in the late Proterozoic. In response to the initiation of Phanerozoic-type plate tectonics, mantle wedges increased in volume by the change from flat- to high-angle subduction, and simultaneously came to be metasomatized by H_2O-rich fluids (Fig. 9b).

2 EVOLUTION OF THE MANTLE THROUGH TIME

It is well-known that the Earth has undergone some major processes since its formation; formation of metallic core, degassing, extraction of continental crust, and differentiation of the silicate mantle. Therefore, it is also necessary to decode the complex events in the Earth's long-term evolution for an investigation of the present-day chemical and physical states of the mantle and continental crust. Working models of present-day mantle dynamics were proposed in the early 1980s after accumulation of geochemical data of mantle-derived rocks and continental crust including Sr and Nd isotopic geochemistry (e.g., Allègre, 1982). In the mid-1980s, the compositional diversity of the mantle was compiled from the compositions of oceanic basalts and continental crust in terms of chemical geodynamics (Zindler and Hart, 1986). In the 1990s mantle tomographies displayed material circulation within the mantle (e.g., Fukao et al., 1992). The combination of geochemical dynamics, mantle tomography and surface geology contributed to establishment of the concept of plume tectonics beyond plate tectonics, and large-scale views of the present mantle (Maruyama, 1994). This section presents our recent studies of the compositional and thermal evolution of the mantle which were the main controls on the evolution of mantle dynamics and surface tectonics through time.

It is important to unravel the evolution of the mantle for an investigation of the geodynamic evolution of the earth because the mantle occupies about 80% of the volume of the whole earth. However, the isotopic evolution of the Earth has been relatively well studied (e.g., Allègre et al., 1980; Galer and Goldstein, 1991; McCulloch and Bennett, 1994), but the thermal evolution of the Earth has not been so well investigated, except for some computational calculations (e.g., Richter, 1985; Davies, 1992; Ogawa, 1997). It was widely accepted in the pre-1970s that the Earth has evolved in an almost steady thermal state, because it was thought that the rate of heat loss from the earth would be similar to the rate of heat production in a chondritic earth (Urey, 1956; Birch, 1958; Tozer, 1965). However, in the 1980s, revised estimates, incorporating correction of the heat loss from oceanic regions, indicated that the heat loss from the Earth is about 30% higher than steady state heat flow from a chondritic earth (Davies, 1980; Pollack, 1980; Sclater et al., 1980). Much geological evidence was also reported for and against the steady state thermal evolution of the Earth. The evidence includes (1) the correspondence of the geothermal gradient of the Archean-aged continental lithosphere to that of Phanerozoic continents (Burke and Kidd, 1978), (2) similarity of the metamorphic facies series between Archean and younger rocks (Windley, 1976; Watson, 1978), (3) the similar height of the mountains in the Archean and at present (England and Bickle, 1984), and (4) presence of the Archean-aged diamonds in kimberlites (Richardson et al., 1984). The counterevidence is the eruption of extremely high temperature magmas of ultramafic komatiitic composition (Green et al., 1975). In the 1990s computer simulations suggested the presence of instability in mantle convection at the Archean-Proterozoic transition, and an episodic or intermittent cooling model of the mantle was highlighted (e.g., Breuer and Spohn, 1995; Davies, 1995). The episodic whole mantle convection model was

also supported by some geological evidence; compilation of U/Pb zircon ages of juvenile continental crust (Condie, 1998, 2000) and of detrital zircons (Rino et al., 2004), secular change of Nd isotopes of greenstones (McCulloch and Bennett, 1994), and geochemistry of different-aged magmas including Nd isotopes, trace elements, rare gas and Pb isotopes (Stein and Hofmann, 1994).

2.1 The secular change of the potential temperature and composition of the MORB source mantle

In the 1990s the potential mantle temperature of the Archean mantle was estimated from the composition of peridotitic komatiites and was higher by 600°C than that of modern MORB (e.g., Takahashi, 1990; Nisbet et al., 1993). However, it is now widely accepted that komatiite was not produced from normal upper mantle, but from plume source mantle or highly wet mantle (e.g., Takahashi and Scarfe, 1985; Campbell et al., 1989; Inoue and Sawamoto, 1992; Parman et al., 1997). Therefore, the potential mantle temperature estimated from the komatiite magma does not represent that of normal upper mantle in the Archean. Abbott and others (1994) estimated the secular variation of the temperature of the upper mantle from the composition of greenstones, and found that the mid-Archean upper mantle was about 250°C higher than the modern upper mantle. But, the estimate may not directly refer to the secular change of the normal upper mantle because they used all of the greenstones, which were derived from mid-oceanic ridges, back-arc basins, primitive island arcs and hotspots. Therefore, it is necessary to determine the tectonic setting of mafic volcanism, because it is well-known that the composition of mafic magmas is strongly dependent on tectonic setting. Many recent investigations of the Phanerozoic circum-Pacific greenstone belts reported a close correlation between the tectonic settings of greenstones defined by chemical discrimination diagrams and the field occurrence of the greenstones. For example, Ueda and others (2000) reported that both MORB and OIB affinity-greenstones occur in a Jurassic to Cretaceous accretionary complex of central Hokkaido in Japan, based on whole-rock compositions including high field strength elements (HFSE), rare earth elements (REE), textures, mineral assemblages and the composition of relict igneous minerals and pseudomorphs of magmatic phenocrysts. Moreover, the MORB-affinity greenstones are covered by thick chert-clastic successions, whereas the OIB-affinity greenstones are intercalated with thin-bedded chert and limestone, or occur as a thick slab or block together with chert and limestone blocks in a black mudstone matrix (Ueda et al., 2000). A detailed review of the occurrence of greenstones in other Phanerozoic accretionary complexes was reported by Isozaki et al. (1990). Maruyama and colleagues worked out determination of the tectonic setting of greenstones in the 3.8 Ga Isua supracrustal belt (Komiya et al., 1999), the 3.5 Ga North Pole area (Maruyama et al., 1991b) and the 3.3 Ga Cleaverville area (Ohta et al., 1996) by comparing them with Phanerozoic greenstone belts. Another inherent problem in geochemical investigations of Archean greenstones is the effect of alteration on original rock compositions. To overcome this problem, it is necessary

to recognize the geochemical effects of such alteration processes as seawater interaction or regional metamorphism prior to any petrographic interpretations as well as to compare the whole rock chemistry with the composition of relict igneous minerals (Komiya et al., 2002c; Komiya et al., 2004).

Figure 10 shows the thermal and compositional evolution of the mantle, estimated by comparing mafic magmas of five different ages with recent melting experiments and multiple saturation experiments of 3.5 Ga MORB from Pilbara (Komiya, 2004). The potential temperature of the source mantles was estimated to be 1480 ± 100 for 3.8 Ga, 1490 ± 70 for 3.5 Ga, 1410 ± 90 for 3.3 Ga, 1500–1566 for 2.5 Ga, and 1470–1500°C for 1.9 Ga mantle and the FeO contents were about 10 wt% . Firstly, the Archean upper mantle potential temperature was only about 100–200°C hotter than the modern equivalent mantle. The estimated temperature is much lower than previous estimates of 1900°C, because they used the composition of peridotitic komatiite for the calculations (Takahashi, 1990; Nisbet et al., 1993). Secondly, the secular variation of the potential mantle temperature of the upper mantle implies that the temperature of the upper mantle has not decreased monotonously but episodically or variably. Although the estimate still has a large error, the potential mantle temperature remained constant from 3.8 to 2.5 Ga, at about 150°C higher than the modern. Moreover, the potential mantle temperature appears to have been lower at 3.3 Ga, whereas it was higher at 2.5 Ga. The thermal variation is possibly consistent with the wide

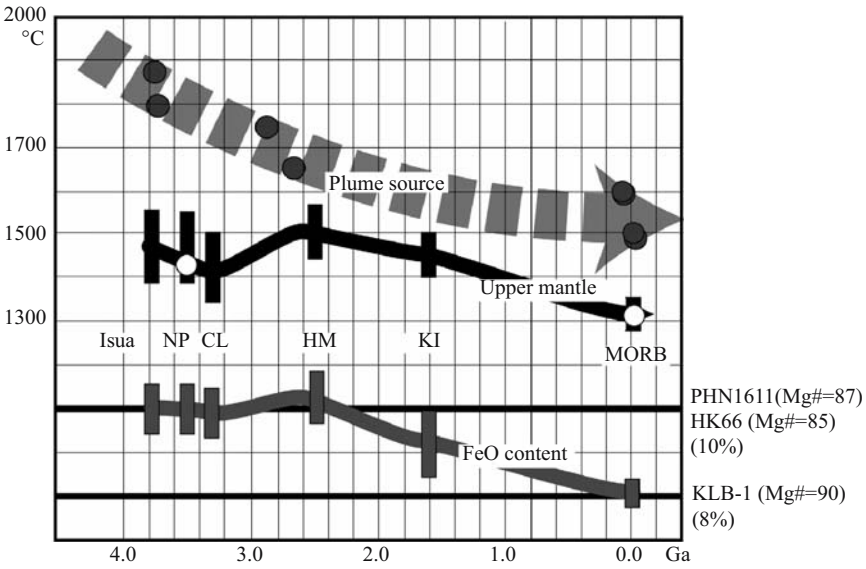


Figure 10. Secular changes of potential mantle temperature (black line) and FeO content (gray line) of the upper mantle, along with potential mantle temperature of a plume source (light gray line, Takahashi, 1990; Nisbet et al., 1993; Sakurai et al., 2001). The left vertical axis represents the potential temperature of the mantle, whereas the right vertical axis represents the FeO content of the upper mantle.

distribution of continental crust (Condie, 1998) and of komatiite rocks (Arndt and Nisbet, 1982) at 2.7 Ga. A steady state of potential mantle temperature through the Archean may be because the hotter lower mantle materials were injected episodically or continuously into the upper mantle. Stein and Hofmann (1994) suggested that the lower mantle material episodically penetrated into the upper mantle because the εNd value of the upper mantle is maintained between primitive and depleted mantle values. In addition, mantle overturn and episodic whole mantle convection is the mechanism suggested by computer simulations (Breuer and Spohn, 1995; Davies, 1995). Although further investigation will be required for the quantification of mantle overturn and the accompanied rejuvenation of the upper mantle, the constancy of potential mantle temperature of the upper mantle also implies episodic whole mantle convection.

2.2 Material circulation model including chemical differentiation and thermal and compositional evolution of the mantle

It has long been thought that the Archean mantle underwent double-layered convection because of the high Rayleigh numbers due to high temperature. In the Archean when the potential mantle temperature was higher by at least 150°C, the viscosity of the mantle became about one-third compared with that of the modern mantle. As a result, the Rayleigh number was about 30 times higher than at present based on the relationship between viscosity and temperature (Honda, 1995). A high Rayleigh number is more compatible with double-layered mantle convection than whole mantle convection (Yuen et al., 1994). In addition, the difference between the depth of phase changes of the subducted basalt and the ambient mantle increases in the hotter mantle (Fig. 11). The combination of these factors suggests that it was more difficult for slab materials to fall down to the lower mantle, and that double-layered mantle convection was preferred rather than whole mantle convection in the Archean. However, whole mantle convection with periodic penetration of subducted materials into the lower mantle is considered to be dominant at present (Fukao et al., 1992), and the mode of the mantle convection is not only controlled by the temperature of the mantle but also by the fate of the accumulated slab. In other words, periodic collapse of an accumulated slab down to the lower mantle causes whole mantle convection (e.g., Maruyama, 1994). Therefore, we can consider whether the intermittent penetration of slab materials into the lower mantle occurred even in the Archean. A higher temperature of mantle in the Archean led to increase of the depth and volume of melting, and thus to a thicker oceanic crust, ca. 15–20 km. On the other hand, the hotter mantle resulted in small plates, and consequently the life-span of oceanic plates was shorter, in order to enable efficient release of the heat flux (Hargraves, 1986; de Wit and Hart, 1993). If the temperature of the mantle were higher by 150°C, about 15 m.y. and 30 km are estimated for the life-span and thickness of the oceanic lithosphere, respectively (Hargraves, 1986; Komiya et al., 1999). Generally speaking, subducted oceanic crust could not penetrate directly into the lower mantle, because basaltic materials change into high-pressure phases at depths of about 40 km greater than the

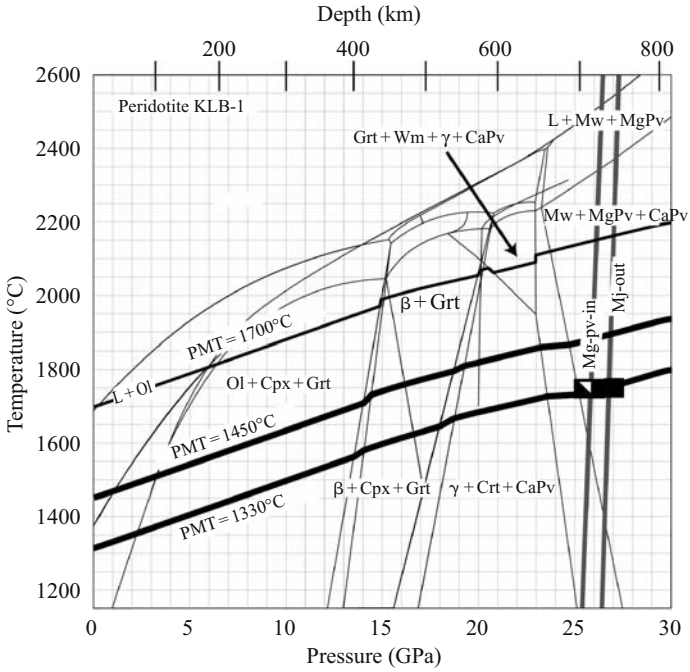


Figure 11. Phase relations of anhydrous peridotite KLB-1 (fine black lines, modified after Figure 1 of Herzberg and Zhang (1996)) and anhydrous Archean MORB (thick gray lines, Hirose et al., 1999). Symbols are defined as follows: L, liquid; Ol, olivine; Opx, orthopyroxene; Cpx, clinopyroxene; Grt, garnet; Mw, magnesiowüstite; MgPv, Mg-perovskite; CaPv, Ca-perovskite; ß, modified spinel (Mg, $Fe)_2SiO_4$, γ, spinel (Mg, $Fe)_2SiO_4$. Also shown are P-T paths of uprising mantle with 1330, 1450, and 1700°C in potential mantle temperature.

ambient peridotite (Hirose et al., 1999). Figure 11 shows the phase relations of KLB-1 in 0–30 GPa, and 1200–2600°C (modified after Herzberg and Zhang, 1996). The P-T paths of the mantle with three different potential mantle temperatures are also drawn: 1330°C (modern upper mantle), 1450°C (the Archean upper mantle) and 1700°C (Archean plume source mantle). The P-T condition of phase change from majorite (Mj)- to perovskite (Pv)-bearing oceanic crust is also shown based on experimental data of Hirose et al. (1999). Although the depth of the upper-lower mantle boundary (ULB) decreases with the potential temperature of the mantle, the difference of potential mantle temperature by 150°C plays an insignificant role on the depth of ULB, by only ca. 7 km (Fig. 11). The high potential mantle temperature of plume source mantle in the Archean promoted upwelling of plumes from the lower mantle (Hirose, 2002), and induced materials in the lower mantle to pass into the upper mantle. By the way, larger quantities of subducted oceanic crust accumulated on the upper-lower mantle boundary in the Archean, because the production rate of oceanic plates was ca. 10 times higher than at present. In particular, significant amounts of subducted

materials built up beneath large continents in the late Archean and early Proterozoic, analogous to the Eurasian continent at present (Engebretson et al., 1992). Assuming that isostasy was valid, the base of a megalith starts to sink into the lower mantle when it grows up to 80 km thick, as estimated from the density contrast between the ambient mantle and subducted basaltic crust (e.g., Irifune and Ringwood, 1987; Hirose et al., 1999). A simple calculation based on the thickness of the oceanic crust and the life-span of the oceanic lithosphere indicates that it took only 100 m.y. for 80-km thick subducted oceanic crust to be stored at the upper-lower mantle boundary in the Archean. In addition, normative calculations of the residue of hydrated basaltic crust after the slab melting suggest that it possibly changes into CaPv + Mj + γ-spinel phases instead of Mj + CaPv + stishovite phases. The residue is heavier than the ambient mantle because of its high concentration of CaPv. There is another remarkable difference between mantle geodynamics in the Archean and at present: the temperature of plume-source mantle. The potential mantle temperature of an Archean plume source mantle reached about 1700°C, but that of modern plume source mantle is about 1500°C. Assuming adiabatic decompression of the plume mantle, the temperature of the former was about 2100°C at 23 GPa and the temperature of the latter is 1900°C. Instead of Mw + MgPv + CaPv, a field of Mj + Mw + γ-spinel + CaPv is present at the higher temperature than about 1950°C at 23 GPa (Fig. 11), and strongly influences the upwelling of the plume-source mantle (Hirose, 2002). A Clapeyron's slope of phase change from Mj + Mw + γ-spinel + CaPv to Mw + MgPv + CaPv is positive, and results in acceleration of upwelling of superplume from lower mantle. Therefore, extensive exchange between upper and lower mantle materials possibly took place in a transition zone from 20 to 24 GPa in the Archean. Seen from the viewpoint of the material exchange, the Archean mantle comprised three layers of upper mantle, transition zone, and lower mantle under the high temperature condition. In addition, if the temperature of the plume-source mantle was higher than 2100°C at 20 GPa, the upwellings of the superplume accelerated at the phase change from ß-spinel + Mj to Mj + Mw + γ-spinel + CaPv, again. As a result, the episodic whole mantle convection was induced by upwelling of superplume. These facts suggest that episodic whole mantle convection, caused by the upwellings of the superplume and collapse of cold subducted materials, operated in the Archean, too.

There may be four plausible mechanisms for the decrease of FeO content through geologic time: core-pumping (Cohen et al., 1980; Dupré and Allègre, 1980); formation of continental crust (e.g., Allègre, 1982); storage of FeO-rich oceanic crust within the mantle (Chase and Patchett, 1988); and iron segregation from the subducted oceanic crust at slab penetration into the lower mantle (this work). However, the core-pumping model is inconsistent with the constancy of compatible siderophile elements such as Ni content through time (Arndt, 1991), and with the abundance of highly chalcophile elements (Newsom et al., 1986). The formation of the continental crust and the storage of the FeO-enriched oceanic crust decrease all lithophile elements including Al_2O_3 and CaO, and are inconsistent with the decrease of only the FeO content. We will discuss below the model of iron segregation from the

subducted oceanic crust at slab penetration into the lower mantle. Recent ultra-high-pressure experiments of natural peridotite and aluminous Mg-perovskite under lower mantle conditions showed that the iron content in Mg-perovskite increases through the coupled substitution of $Al^{3+} + Fe^{3+} = Mg^{2+} + Si^{4+}$ with Al_2O_3 (Wood and Rubie, 1996; McCammon, 1997). Moreover, some ferrous ions were transformed into metallic iron by an electron exchange reaction of $3Fe^{2+} = Fe + 2Fe^{3+}$ accompanying the substitution reaction of $Al^{3+} + Fe^{3+} = Mg^{2+} + Si^{4+}$ (McCammon et al., 1997; Frost et al., 2004). The reactions occur during slab penetration into the lower mantle because the subducted oceanic crust contains high Al_2O_3 and FeO content. Especially, in the Archean, the chemical differentiation by the reactions was more significant because the production rate of oceanic crust in the Archean was higher by 10 times than at present. However, Sun (1984) emphasized that the metallic core has not grown after the Archean, based on the ratio of siderophile to lithophile elements such as the P_2O_5/TiO_2 ratio. Although his work compared Precambrian komatiite and picrite magmas with modern NMORB, comparison between Archean and modern MORB indicates an obvious secular variation of the P_2O_5/TiO_2 ratio (Komiya, 2004). In addition, Hofmann and others (1986) showed that Ce/Pb ratios of modern MORB and OIB are higher than those of the primitive mantle. The high ratio of Ce/Pb of modern MORB and OIB relative to that of the primitive mantle is consistent with the extraction of metallic iron from subducted oceanic lithosphere during slab penetration, if source mantles of MORB and OIB involve residual materials after segregation of metallic iron. Therefore, extraction of metallic iron is consistent with a secular change of incompatible siderophile elements. On the other hand, there are no obvious secular variations of compatible siderophile elements such as NiO (e.g., Arndt, 1991). A difference of behavior between compatible and incompatible siderophile elements can be explained by a difference between the abundance of the compatible elements in the oceanic crust and mantle peridotite, and by the partition coefficients at high pressure. The physicochemical difference between siderophile and lithophile elements, in general, decreases under ultrahigh pressure conditions, and partition coefficients of P and Ni between metallic and silicate liquids decrease to ca. 3.1 and 40 at 27 GPa, 1400°C, $\Delta IW = +2$ (Righter et al., 1997). Also, the NiO content in the oceanic crust is lower by a tenth than in the mantle (e.g., McDonough and Sun, 1995). Therefore, the segregation of metallic iron plays a significant role in the abundance of incompatible siderophile elements such as P, but an insignificant role in the abundance of compatible elements.

Here, we estimate the amount of metallic iron precipitated from subducted oceanic crust during slab penetration into the lower mantle using the parameters given by Komiya (2004). The calculation indicates that assuming that the production rate of metallic iron is half of the production rate of ferric iron, it takes only 3.1 b.y. to reduce the FeO content in the whole mantle from 10.2 to 8.1 wt% at the production rate of MORB in the Archean; and the phosphorus content of the whole mantle also falls from 29 to 21 ppm in only 5 b.y. However, no secular change appears in the NiO content because the NiO content of the whole mantle decreases by only 0.02 wt% in 5 b.y.

This line of evidence indicates that chemical differentiation occurs at the upper-lower mantle boundary, and that a model of iron segregation from subducted oceanic crust during the slab penetration into the lower mantle is plausible to decrease in the FeO content and incompatible siderophile elements in the mantle. If the produced metallic iron sinks and is accumulated on the core, the thickness of the layer of metallic iron would be about 57 km.

Recent ultrahigh-pressure experiments suggested differentiation of subducted oceanic crust at a subduction zone, at the upper-lower mantle and core-mantle boundaries within the mantle as shown in the preceding sections. For example, Hirose and others (2004) suggested that subducted basaltic crusts are molten into denser FeO-rich picritic melt and lighter residue that exists on the core-mantle boundary, and that fractionations of U to Pb and of Lu to Hf occurs because the dense FeO-rich melt accumulates on the core-mantle boundary, whereas the light residue rises toward the upper mantle. However, many current models of material circulation within the mantle suppose that subducted materials do not change within the mantle, and that the mode of the material cycling is immutable through time.

Figure 12 shows the view for global material cycling through time, including chemical differentiation of the subducted materials within the mantle. In the Archean, oceanic lithosphere was thinner, and had a thicker oceanic crust and a shorter life span because of the higher potential mantle temperature. In addition, there were many subduction zones, namely plate boundaries, because the size of plates was smaller. A high geothermal gradient at subduction zones resulted in partial melting of subducted oceanic crust, and changed the oceanic crust into a denser garnet-bearing residue. As a result, large amounts of oceanic crust subducted into the deep mantle and accumulated on the upper-lower mantle boundary. The accumulated materials delaminated at the bottom, and subsided into the lower mantle. Iron grains were segregated from the slab materials during the slab penetration into the lower mantle, and subsided onto the core-mantle boundary. On the other hand, some of the residue was mixed with the surrounding mantle, and other materials sank to the core-mantle boundary. On the core-mantle boundary, the subducted oceanic crust was partially molten, and differentiated into a dense FeO-rich picritic melt and light Ca-perovskite-bearing residue (Hirose et al., 2004). The FeO-rich melt accumulated on the core-mantle boundary, whereas the light Ca-perovskite-bearing residue rose to the upper mantle. The upper-lower mantle boundary intermittently opened during subsidence of slab materials into the lower mantle and enabled injection of superplumes from the lower to the upper mantle. In the Phanerozoic, oceanic lithospheres have become thick and wide, whereas the oceanic crusts are thinner. As a result, the subducted oceanic crust in the Phanerozoic plays a less significant role in the chemical differentiation than in the Archean. Most oceanic crust undergoes dehydration instead of slab melting at a subduction zone, except for very young oceanic plates. Subducted materials accumulate on the upper-mantle boundary, and produce megaliths, which continually sink into the lower mantle, whereas superplumes rise up to the upper mantle from the core-mantle boundary.

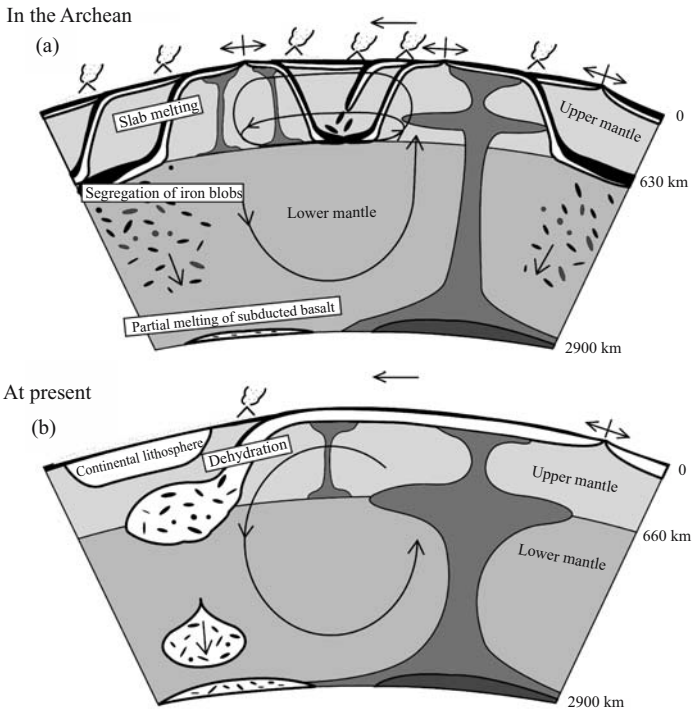


Figure 12. Cartoons of material circulation in the whole mantle in the Archean (a) and in the Phanerozoic (b). In the Archean, thin oceanic lithosphere with thick oceanic crust subducted beneath small oceanic island arcs in many places, and slab materials were widely distributed over the upper-lower mantle boundary. The high production rate of Archean MORB probably resulted in successive subsidence of slab materials into the lower mantle. The formation of the continental crust at subduction zones by slab melting and segregation of iron blobs during slab penetration into the lower mantle have changed the chemical composition of the mantle through geologic time. Partial melting of the subducted oceanic crust on the core-mantle boundary also possibly plays a significant role in the compositional change of the mantle (Hirose et al., 2004). In the Phanerozoic the thick oceanic lithosphere with thin oceanic crust subducts beneath large continental blocks. A huge amount of slab material accumulates beneath a large continent for a long time, and continually subsides into the lower mantle (Fukao et al., 1992).

3 MAJOR EPISODIC INCREASES OF CONTINENTAL CRUSTAL GROWTH AND IMPLICATIONS FOR MANTLE OVERTURNS IN THE EARLY PRECAMBRIAN

The present surface of the Earth is covered with 70% oceanic crust and 30% continental crust. The oceanic crust is basaltic and 0.8–11 km thick, whereas plume-affected crust may be up to 38 km thick (Gladczenko et al., 1997). In contrast, continental crust is about 30–40 km thick, and composed of a felsic to intermediate upper crust and

a basaltic lower crust. The differences in thickness and density between the oceanic and continental crusts result in a unique topographic expression. Earth has a bimodal topographic frequency of elevation, whereas Venus has only one predominant elevation (Phillips et al., 1981). Also, the moon has a bimodal topographic elevation, and a very thick, up to 75 km, continental crust, but its continental crust is anorthositic, dissimilar to the sialic continental crust of the Earth. The moon's anorthositic crust was formed by igneous differentiation of a magma ocean at its birth (Warren, 1985). These relations indicate that the presence of a sialic continental crust is one of the unique characteristics of the Earth. For these reasons, it is important to study the origin and growth rate in order to understand the evolution of the solid Earth (Fowler et al., 2002).

At present, the oldest oceanic crust has an age of about 200 Ma, and is present in the western Pacific and the Atlantic. However, many fragments of oceanic crust were emplaced within accretionary complexes during off-scraping and underplating of oceanic material at the trench (e.g., Isozaki et al., 1990), and fragments of Precambrian oceanic crust also exist in ancient accretionary complexes (e.g., Komiya et al., 1999). In contrast, the oldest sialic continental crust of the earth is ~4.03 Ga orthogneiss in the Acasta Gneiss Complex in the Northwest Territories of Canada (Bowring and Williams, 1999). The oldest minerals in the world are ca. 4.4 Ga detrital zircons from conglomerates of Jack Hills in the Yilgarn craton, western Australia (e.g., Wilde et al., 2001). The rare earth element (REE) patterns and Hf isotopic composition of the zircons indicate that they were derived from continental felsic magma (Kinny et al., 1991; Maas et al., 1992). Recently, oxygen isotope and titanium concentration of the zircons indicate that the parental magma was granitoid, formed from hydrated materials (Cavosie et al., 2005; Watson and Harrison, 2005). This line of evidence indicates that significant continental granitic crust had already formed in the Hadean soon after formation of the Earth. Kamber et al. (2003) argued that preservation of >3.8 Ga material is restricted to cratons with a high U/Pb source character (North Atlantic, Slave, Zimbabwe, Yilgarn and Wyoming), and that the Pb-isotope systematics of these cratons result from reworking of material that was derived from ca. 4.3 Ga Hadean, basaltic crust. We reinvestigated the geology, geochronology and geochemistry of the Acasta Gneiss complex because ancient crustal rocks provide the only direct evidence for evolution of the surface environment and solid earth in the Hadean and Early Archean. We recognized six distinct lithofacies, and at least eight tectonothermal events based on 1/5000 scale geological mapping, detailed study of many outcrops and petrographic investigation of ca. 1000 samples (Komiya et al., 2002b; Iizuka et al., 2006). It mainly comprises early Archean Gray (GG), White (WG) and Layered (LG) Gneisses and middle Archean Foliated Granite (Fig. 13a). GG originated from quartz-diorite, and occurs as enclaves within the WG and LG, which were originally pale-gray tonalitic and white granitic rocks. The gneissic structure of WG is concordant with the shape of the included GG blocks, but completely discordant to those within the GG. The intersection relationship indicates that the GG is older than the well-dated WG (4.0 and 3.7 Ga). In addition, we classified separated zircons into primary, inherited and recrystallized types most effectively using

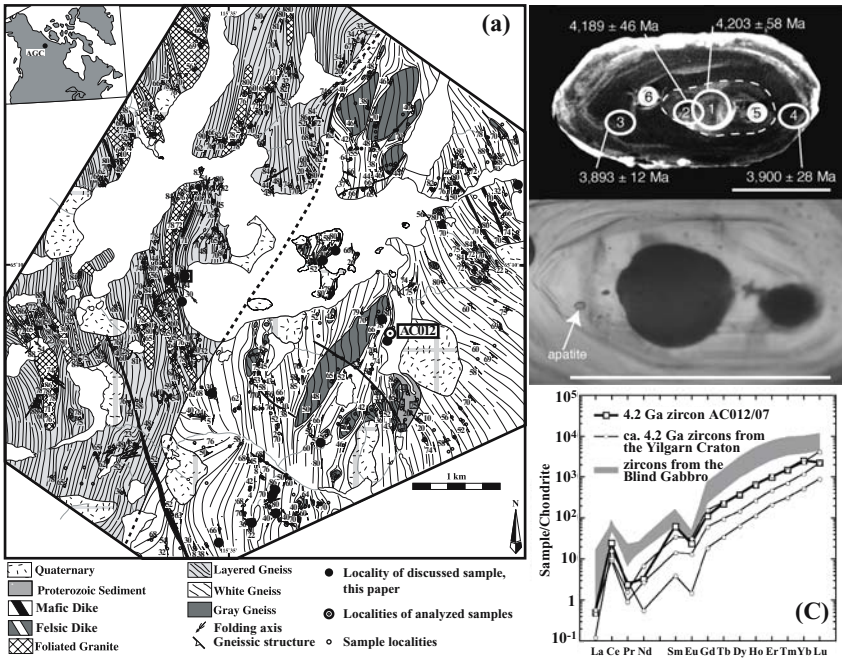


Figure 13. (a) A geological map of the Acasta Gneiss Complex, comprising six distinct lithofacies. (b) A cathodoluminescence image of a zircon with a 4.2 Ga inherited core containing an apatite inclusion. (c) An REE pattern of the inherited core, indicating the host magma was quartz-dioritic.

the Cathodoluminescence (CL) images (Iizuka et al., 2006). The REE patterns of primary zircons within the WG are consistent with those of the host whole rock. The inherited zircons are much older, up to 4203 ± 58 Ma (Fig. 13b), and have REE patterns equilibrated with quartz-dioritic magma based on the discrimination methods (Fig. 13c). The result indicates that the oldest rocks are the 4.2 Ga quartz-dioritic enclaves within the WG, that, when formed, was accompanied by recycling of some portion of the preceding GG. The discovery of the Hadean zircons and wide distribution of quartz-dioritic enclaves in the Acasta Gneiss Complex, including detrital (Wilde et al., 2001) and inherited zircons (Nelson et al., 2000) in the Narryer Complex, implies extensive distribution of continental crust even in the Hadean, consistent with early differentiation of the upper mantle (Bennett et al., 1993).

Many different models of continental growth have been proposed, and can be classified into three groups, according to their methods of estimate and the feature (Fig. 14). The first involves rapid continental formation in the Hadean and Early Archean based on a thermal evolution model and estimate of net growth of continental crust in the Phanerozoic (Fyfe, 1978; Armstrong, 1981; Reymer and Schubert, 1984). Armstrong (1981) first emphasized the significance of recycling crustal materials into the mantle.

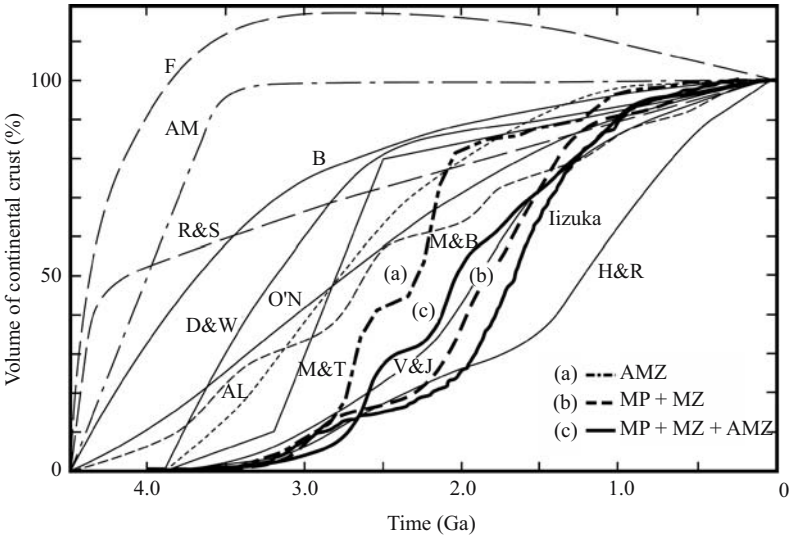


Figure 14. Growth rate estimated from the age population of detrital zircons in the river sands along with crustal growth curves from the literature (Rino et al., 2004); MP, MZ and AMZ represent continental growth rate in the drainage of the Mississippi, Mackenzie, Amazon Rivers, respectively. Iizuka (Iizuka et al., 2005), H & R (Hurley and Rand, 1969), C (Condie, 1998), V & J (Veizer and Jansen, 1979), M & T (McLennan and Taylor, 1982), AL (Allègre, 1982), O'N (O'Nions et al., 1979), M & B (McCulloch and Bennett, 1994), R & S (Reymer and Schubert, 1984), D & W (Dewey and Windley, 1981), B (Brown, 1979), Am (Armstrong, 1981), F (Fyfe, 1978). The continental growth curves are different between the continents. The summarized continental growth curve of two continents indicates episodic growth of continental crust at ca. 2.7 and 2.0 Ga.

According to his model a high proportion of continental crust was produced before the Archean, so that the proportion remained practically constant in later time due to recycling. Reymer and Schubert (1984) estimated the amount of subduction erosion of continental and oceanic materials, and the net amount of continental growth in Phanerozoic subduction zones. They concluded that the net amount of continental growth was small in the Phanerozoic, and suggested that the continental crust was largely produced in the Archean. The second group advocates gradual continental growth since the Archean, and significant growth in the Phanerozoic. These models were made on the basis of the present distribution of the continental crust and its ages (Hurley and Rand, 1969; Condie, 1998). For example, Hurley and Rand (1969) measured the whole-rock Rb-Sr isotopic compositions of the juvenile continental crust in North America, and estimated the continental growth rate from their distribution and their radiometric ages. Condie (1998) compiled the distribution and recent U-Pb zircon ages of juvenile continental crust, and showed a gradual growth of continental crust since the Archean with a few periods of rapid growth of continents. The third group is characterized by the formation of a significant amount of continental crust by

the Archean, and subsequently a gradual increase (Moorbath, 1977; O'Nions et al., 1979; Allègre, 1982; McCulloch and Bennett, 1994). These models were based on the isotopic evolution of the mantle estimated from the geochemistry of greenstones of different ages.

In order to better understand the continental growth history, we have determined the U-Pb age of about 1500 detrital zircons from river sands in three major rivers, the Mississippi, Mackenzie, and Amazon Rivers in the North and South America continents (Fig. 14; Rino et al., 2004). The method for estimating continental growth from the age population of a significant number of detrital zircons in river sands has three advantages (Rino et al., 2004): (1) the almost even collection of zircons from sedimentary rocks and granitic basements in the hinterlands of the major rivers; (2) determination of the age of juvenile crust due to the high closure temperature of the U-Pb systematics of zircons, and the removal of the influence of recycling of crustal materials; and (3) direct determination of the age of continental formation. The processes of recycling of continental materials are classified into three types: intra-crustal recycling, remelting of continental materials and subduction of continental materials into the mantle. Especially, this method is potentially useful for eliminating the effect of intra-crustal recycling. Our estimated continental growth curve displays two clear sudden increases at 2.8–2.5 and 2.3–2.0 Ga (Rino et al., 2004). The discontinuous growth of continental crust indicates episodic crustal growth, because this method minimizes the influence of recycling of crustal materials, and because zircons are almost evenly gathered from the drainage regions. In addition, the result clearly shows that timing and scale of continental growth were different among the continents because age distribution of zircons is different between the North and South American continents. In contrast, extensive continental formations in the Late Archean and early Proterozoic are common in the North and South American continents, which imply global events as shown below.

Iizuka et al. (2005) made in-situ analyses of U-Pb ages and $^{176}Hf/^{177}Hf$ isotopic ratios of over 400 grains of detrital zircons in the Mackenzie River by laser ablation-inductively coupled plasma mass spectrometry (LA-ICPMS). The purpose of the study was to consider the second type of recycling, remelting of continental materials. The U-Pb isotopic data for 416 igneous zircons are summarized in a histogram (Fig. 15b), that shows three peaks, a low 2.6–2.8 Ga peak, a broad 0.9–1.8 Ga peak, and the highest sharp <0.2 Ga peak. The initial $^{176}Hf/^{177}Hf$ isotope ratios for 402 grains of the 416 dated zircons are plotted along with chondritic uniform reservoir (CHUR) and DM evolution curves (Fig. 15a). The DM evolution curve was defined by $(^{176}Hf/^{177}Hf)_i = 0.279724$ and $^{176}Lu/^{177}Hf = 0.0395$, which is consistent with the mean value of the MORB field (0.28323; Nowell et al., 1998) and the initial Hf isotopic composition of the 2.7 Ga juvenile rock (0.28119; Vervoort and Blichert-Toft, 1999). To evaluate the degree of depletion of its parental magma relative to DM, the $\varepsilon Hf(T)_{DM}$ was calculated. Moreover, we calculated mantle extraction model ages (T_{DM}) for all grains, assuming that the parental magmas of the zircons were produced from crustal materials that were originally extracted from the DM, and that the Lu/Hf ratio of the crustal reservoir was the ratio of the upper continental crust

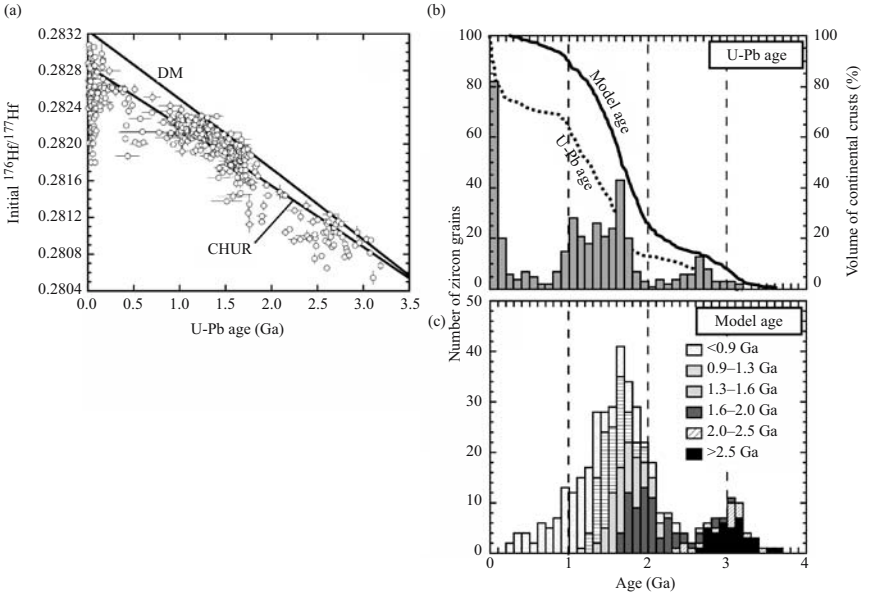


Figure 15. (a) Plot of initial $^{176}Hf/^{177}Hf$ vs. U-Pb age for 402 analyzed zircon grains. For the calculation of initial Hf isotope ratio, the decay constant for ^{176}Lu proposed by Scherer et al. (2001) (1.865×10^{-11} yr^{-1}) was used. CHUR evolution curve is based on CHUR parameter proposed by Patchett et al. (2004). Histograms of U-Pb age of 416 zircon grains (b), and T_{DM} of 402 zircon grains (c). The continental growth curves based on U-Pb age and T_{DM} are also illustrated in (b).

(Lu/Hf = 0.055; Taylor and McLennan, 1985). The histograms of T_{DM} population and the continental growth curves estimated from U-Pb age and T_{DM} population are shown in Figure 15b, c. Figure 15 show that many zircons have negative $\varepsilon Hf(T)_{DM}$, and indicate that the source materials underwent remelting of crustal materials. The highest $\varepsilon Hf(T)_{DM}$ values are scattered along the DM evolution curve, but deviate at some points. The deviation implies that DM was frequently refertilized through time. The continental growth rate in the drainage based on the T_{DM} population indicates that 15% and 78% of the present continental crust were formed by 2.5 and 1.3 Ga, respectively (Fig. 15b). In addition, it also demonstrates that crustal recycling became more significant with time, and $\varepsilon Hf(T)_{DM}$ of all the Phanerozoic zircons have quite a large negative anomaly. Figure 15a, c show that some zircons have negative $\varepsilon Hf(T)_{DM}$ even in the Archean. The T_{DM} of >2.5 Ga zircons range between 2.7 and 3.6 Ga. The Mississippi River drains the Archean Wyoming Craton and western Superior Provinces. The Wyoming Craton comprises abundant metasedimentary rocks, and possesses isotopic evidence for the presence of Middle Archean or older continental crust (Wooden et al., 1988; Frost, 1993). In addition, the granitoids in the craton were formed at 2.55–2.8 Ga, but their Nd model ages are 2.7–3.4 Ga, indicating both formation of some juvenile crust and recycling of older crust at the time (Frost et al.,

1998). On the other hand, continental and oceanic crustal fragments with 2.66–3.2 Ga ages occur in the western Superior Province, and the Nd isotopic data of the felsic volcanic and plutonic rocks also indicates both juvenile crustal formation and recycling of ~3.4 Ga crust (Tomlinson et al., 2004). The T_{DM} data support the previous isotopic studies, which suggest that crustal formation even in the Archean resulted from both the formation of juvenile continental crust and the recycling of older crustal materials. The comparison between the U-Pb age and the T_{DM} population shows firstly that significant Phanerozoic continental growth in the U-Pb age population was not observed in the T_{DM} (Fig. 15c). This fact indicates that most Mesozoic to Cenozoic crusts, at least in the drainage of the Mississippi River, originate from old crustal materials. Secondly, Figure 15c shows that the T_{DM} was predominant between 2.0 and 1.3 Ga, when its proportion reached 53%. This indicates that a huge amount of juvenile crust was formed between 2.0 and 1.3 Ga, and that a significant amount of the crust was subsequently recycled into younger crust. Thirdly, there is no evidence for >3.2 Ga crust in the U-Pb age population, but the T_{DM} histogram shows the existence of early Archean juvenile crust. This indicates that crustal growth started by the early Archean in the drainage basin, but was not preserved except for material in sediments and xenocrysts in younger granitoids. Finally, we emphasize that there is a significant difference between the U-Pb age and T_{DM} histogram, and that crustal recycling was very an important process in continental formation.

After the 1990s, episodic growth models of continental crust came into the limelight (McCulloch and Bennett, 1994; Stein and Hofmann, 1994; Condie, 1995; Davies, 1995; Peltier et al., 1997; Condie, 1998). Condie (2000) suggested that very short-term crustal formation occurred at 2.7, 1.9, and 1.2 Ga. The episodicity of orogeny was originally proposed by Gastil (1960) and Runcorn (1965) from their worldwide compilations of Precambrian isotopic mineral ages. Their age-distributions are supported by recent compilations of mineral ages and the tectonic setting, and explained by episodic thermal activity of the mantle (Barley and Groves, 1992). In addition, some peaks of crustal-age distributions were inferred from the distribution of T_{DM} of juvenile continental crust in the USA (Nelson and DePaolo, 1985), Australia (McCulloch, 1987) and South America (Cordani et al., 2000), from U-Pb ages of zircons (Condie, 1998; Rino et al., 2004), and from Rb-Sr isotope systematics (Hurley and Rand, 1969), and they were interpreted in terms of episodic crustal growth as well as the discontinuous occurrence of the mineral ages (e.g., Moorbath, 1977; McCulloch and Wasserburg, 1979; Nelson and DePaolo, 1985; Stein, 1994 # 207; Condie, 1998; Rino et al., 2004). However, the uneven crustal-age distribution may also be explained by the selective erosional recycling of elevated crust and by the uneven positioning of growth and recycling of continental crust (Gurnis and Davies, 1986; Windley, 2003). We considered the recycling of crustal materials, and quantitatively estimated the rate of continental growth from the U-Pb ages and Hf isotopic compositions of a large number of igneous zircons in river sands as shown above (Rino et al., 2004; Iizuka et al., 2005). The results also indicate significant juvenile continental growth at 2.5–2.8 and 1.8–2.2 Ga. As a result, we shall discuss a mantle overturn hypothesis for the episodic growth of the continental crust.

Several recent geochemical and geological studies have reported anomalous thermal events at 2.7 and 1.9 Ga. Compilation of 304 large igneous provinces (LIPs) since 3.8 Ga showed that the LIPs record is semi-continuous back to at least 3.0 Ga, and there was no obvious periodicity, but that there were apparent increases in plume activity between 0.15 Ga and the present, and between 2.8 and 2.7 Ga (Ernst and Buchan, 2002a,b). Figure 16 illustrates the distribution of LIPs around 2.7–2.8 Ga (references in Rino et al., 2004), and shows that plume activity occurred worldwide. The interpretation of the apparent high distribution of LIPs in the Late Archean is still controversial as to whether it represents an increase of activity of plume magmatism or an exclusive preservation of oceanic LIPs (Ernst and Buchan, 2002b), but the high proportion and worldwide distribution indicate that more active magmatism occurred globally in those days. Many LIPs between 1.9 and 2.1 Ga are also scattered throughout the world. By the way, Maruyama (1994) considered that continental collisions are the herald of subsequent active superplume magmatism, because successive subduction of oceanic materials under a large continent results in the thick accumulation and the formation of a cold plume underneath. Figure 16 also displays late Archean metamorphic belts, and includes collision-type metamorphic belts such as the Limpopo Belt between the Zimbabwe and Kaapvaal Cratons, collisions between the Akulleq, Akia and Tasiusarsuaq terranes in southern West Greenland, and amalgamation of the East and West Pilbara terranes in Australia (references in Rino et al., 2004). In the early Proterozoic, many collisional orogenic belts were also formed. Reconstruction of ancestral supercratons from present cratons based on their

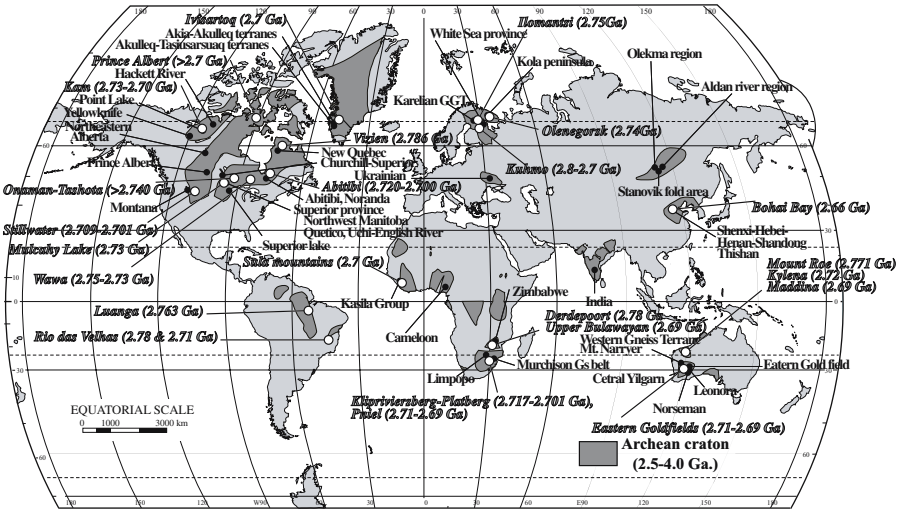


Figure 16. Distribution of large igneous provinces, including continental flood basalts, rift magmatism, komatiitic magmatism, and regional metamorphism between ca. 2.8 and 2.7 Ga (references in Hayashi et al., 2000; Rino et al., 2004). They are scattered in many Archean continents.

geological and geochronological similarities indicates that the cratons can be classified into only a few supercratons in the late Archean and early Proterozoic, when they became relatively large cratons through collision and amalgamation (Bleeker, 2003). This line of evidence suggests that some large continents were formed by collision/amalgamation of cratons and terranes after successive subduction, similar to formation of the modern Eurasian continent, and this implies formation of thick megaliths underneath. The formation of large megaliths in the mantle transition zone and their subsequent collapse causes exchange between upper and lower mantle materials, and influx of fertile and hotter lower mantle materials into the upper mantle. In the Archean, a ca. 150°C hotter mantle resulted in a higher Rayleigh number and an increase of difference of depth of the phase changes between subducted basalt and ambient mantle. In this case, the upper mantle would have behaved as a stagnant lid, and its breakage would have led to a catastrophic mantle overturn because quite large amounts of subducted materials had accumulated before the collapse to the lower mantle. As a consequence, descending slabs would have sunk into the lower mantle (the catastrophic mantle avalanche events of Condie, 1998) and superplumes and plumes would have ascended from the core-mantle boundary to give rise to LIPs (Fig. 17). From our results combined with published data, we suggest that such overturns took place at 2.8–2.6 Ga and at 1.9–1.7 Ga.

The mantle overturn model, which explains the punctuated tectonic evolution of the earth, is based on the thermal evolution of the mantle according to parameterized convection theory. The general model, applied to evolution of the earth, was proposed by McCulloch (1993), developed by Breuer and Spohn (1995) with respect to the Archaean-Proterozoic transition, and constrained by Davies (1995) with numerical calculations. Breuer and Spohn (1995) and Stein and Hofmann (1994) proposed models in which layered mantle convection changes catastrophically to whole-mantle convection during short-lived episodes. The driving forces for such catastrophic movement of mantle materials (mantle overturn) are: thermal instability of the 660 km boundary between cooling upper mantle and lower mantle heated up by radioactive decay (Breuer and Spohn, 1995), and upwelling of a superplume induced by episodic sinking of the accumulated slab materials at the transition zone into the lower mantle (Maruyama, 1994; Stein and Hofmann, 1994; Davies, 1995; Larson and Kincaid, 1996). McCulloch and Bennett (1994) proposed phased growth of a depleted mantle reservoir at the cost of a primitive lower mantle. Compilation of collisional orogenic belts and geological evidence of the presence of large-scale continents at about 2.7 and 1.9 Ga suggests that the mantle overturns were caused by periodic subsidence of subducted oceanic materials under the large continents into the lower mantle.

Mantle overturn was expressed by catastrophic downwelling of cold subducted slabs through the 660-km boundary and by a corresponding upwelling in the form of superplumes from the lower mantle. Where some arose under oceanic plates, they gave rise to oceanic plateaus. The worldwide occurrence of active komatiite magmatism in the late Archean and of OIB-type magmatism in the early Proterozoic (e.g., Stern et al., 1995) supports more active plume-related volcanism at these times (Fig. 16). Where the small plumes arose under a continent, they gave rise to continental

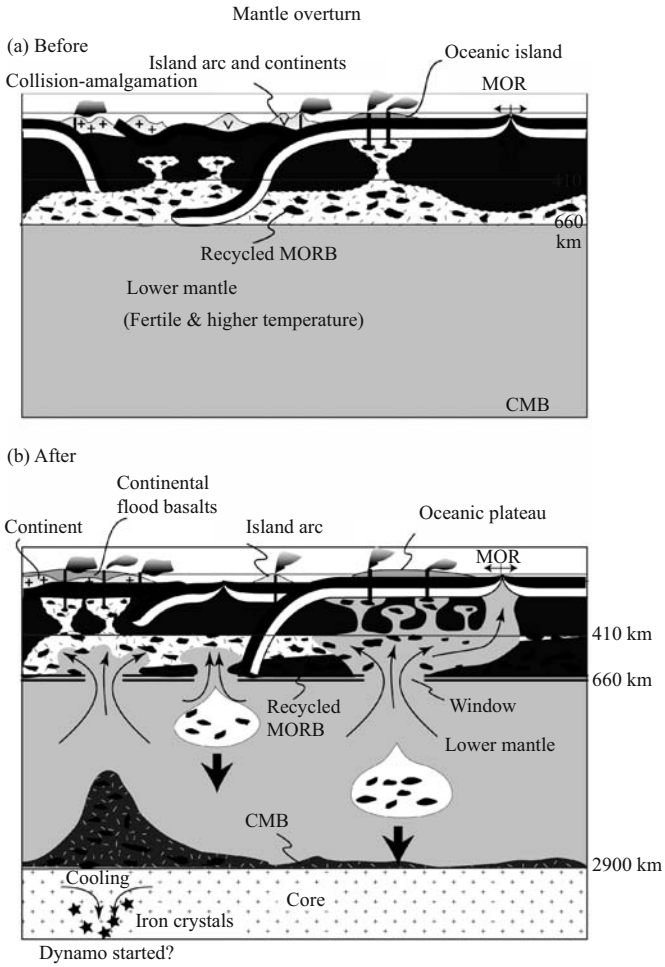


Figure 17. Schematic diagrams of mantle convection systems before and after an overturn (a) In the Archean double-layered convection was dominant because a higher potential mantle temperature of ca. 150°C made the Rayleigh number of the mantle ca. 30 times higher than that of the modern upper mantle. The high potential mantle temperature also resulted in a high productivity of MORB, and accumulated significant amounts of subducted oceanic crust beneath continents. Many island arcs were formed at subduction zones through accretion of oceanic materials and by slab-melting of subducted oceanic basalt to produce TTG magmas. They collided to make continents just before the mantle overturn event. (b) The catastrophic downwelling of the accumulated oceanic crust on the boundary between the upper and lower mantle induced influxes of hotter and more fertile material from the lower mantle. The exchange of materials and the heat transfer between the upper and lower mantle caused active plume-magmatism, and produced large amounts of basalt and komatiite. In addition, continental flood basalts formed on large continents from induced plumes accompanied by entrapment of subducted oceanic crust. After the mantle overturn, the upper mantle became hot and fertile to produce more oceanic crust at mid-oceanic ridges, and consequently more sialic continental crust was formed by partial melting of hydrated basalt at subduction zones.

flood basalts, and cognate mafic dyke swarms (Fig. 16). A recent thermal model of the mantle implies that just before the mantle overturn, the upper mantle was already cooled and depleted so that it could not produce much oceanic crust (Komiya, 2004). Consequently, the productivity of continental crust also decreased at subduction zones at that time. Episodic mantle upwelling gave rise to higher rates of oceanic plate accretion because the influx of hotter and more fertile materials from the lower to the upper mantle produced more basaltic magma at mid-ocean ridges. In this regard, subduction of younger and more oceanic crust led to increased accretion of oceanic materials and/or the slab-melting of them to produce more TTG magmas at subduction zones. This chain of events resulted in formation of more island arcs and episodic continental growth in the Archean.

4 PERSPECTIVE: EVOLUTION OF THE SOLID EARTH AND THE INFLUENCE ON SURFACE ENVIRONMENT

Some elements such as V, Cr, Fe, Ce and Eu have multivalence, and are dependent on their redox state under melting and crystallization conditions. $Fe^{3+}/\sum Fe$ ratio of magma is dependent on the redox state, the temperature, pressure, and composition, and the redox state is the most important among them (e.g., Carmichael, 1991). The oxygen fugacity of the modern upper mantle, especially the MORB-source mantle, ranges around the FMQ buffer, and is estimated from $Fe^{3+}/\sum Fe$ ratios of 0.07 ± 0.03 and 0.023 ± 0.05 for MORB glass and spinel peridotite, respectively (Christie et al., 1986; O'Neill et al., 1993). On the other hand, the $Fe^{3+}/\sum Fe$ ratio of whole rock depends on not only the redox state but also the mineral assemblage (O'Neill et al., 1993; Ballhaus, 1995). For example, peridotite contains little ferric iron because olivine of the major minerals contains no ferric iron, whereas materials in the mantle transition zone have higher $Fe^{3+}/\sum Fe$ ratios because wadsleyite, ringwoodite and majorite contain more ferric iron (O'Neill et al., 1993). Mg-perovskite also contains much ferric iron, simultaneously substituted with aluminum for Mg and Si. As a result, the Fe^{3+}/Fe ratio increases in the deep mantle even at a constant redox state. If lower mantle materials with high $Fe^{3+}/\sum Fe$ ratios ascend to the upper mantle, the upwelling materials have higher ferric iron relative to ambient mantle peridotite, depending on the diffusivity of oxygen or the exchange rate between ferric and ferrous within the mantle. It is widely known that H_2O and CO_2 are easily mobile, but mobility of O_2 or the exchange between Fe^{2+} and Fe^{3+} are restricted (e.g., Chinner, 1960; Mueller, 1960). In addition, there are some mantle materials with the inherited signature of lower mantle materials. For example, clinopyroxenes in xenoliths from Savai'i Western Samoa and Tubuai, Austral islands (Hauri et al., 1993) and from Salt Lake Crater, Hawaii (Salters and Zindler, 1995) inherit trace element patterns from their precursors (Hirose et al., 2004), and some mineral inclusions in lower mantle diamonds have original trace element composition even after phase change from Ca-perovskite to wollastonite (Stachel et al., 2000; Kaminsky et al., 2001). In addition, the lower mantle is inferred to contain 10–20% higher FeO from seismic tomography and mineral physics constraints (e.g., Kellogg et al., 1999), and the fingerprints are still

preserved even after upwelling to the upper mantle and subsequent partial melting (Humayun et al., 2004). These observations imply preserved inheritance of lower mantle conditions even after phase change of minerals because elemental diffusivity is small at the hand-specimen scale. In the case of low diffusivity of oxygen, the materials from the lower mantle would have high oxygen fugacity compared with normal upper mantle because of their high $Fe^{3+}/\sum Fe$. At present, two superplumes arise from the core-mantle boundary in Polynesia and the southern Africa areas. At 2.7 Ga, a mantle overturn event caused upwelling of large amounts of lower mantle materials to the upper mantle. These events possibly oxygenized the upper mantle, and then the surface environment.

Another relevant mechanism is: the mantle was externally oxidized through time. Two different ideas were proposed for the secular change of mantle oxygen fugacity; gradual increase (e.g., Kasting et al., 1993; Eggler and Lorand, 1994; Lécuyer and Ricard, 1999; Kump et al., 2001) and constancy through geological time (Arculus, 1985; Canil, 1997; Delano, 2001). The former estimated the redox state of the mantle from sulfide barometry within peridotitic diamonds from the tectosphere (Kasting et al., 1993; Eggler and Lorand, 1994) and from a box model of the Fe^{3+} cycle between the mantle, subduction zone, continental crust and sediments (Lécuyer and Ricard, 1999). In addition, it is well known that it took half a billion years after emergence of photosynthetic bacteria before a significant amount of O_2 first appeared in the atmosphere. As a hypothesis to account for the delay, oxidation of upper mantle through time is favored, and several models were proposed such as: the upper mantle was oxidized by subduction of hydrated oceanic crust and/or oxidized sediments and the release of reduced volcanic gases (Arculus and Delano, 1987; Kasting et al., 1993). The influx of reduced gases from the ancient reduced mantle suppressed the biological oxygenation of the surface environment that became oxic after the mantle was oxidized (Kasting et al., 1993; Kump et al., 2001). However, the delay can be explained by another mechanisms: an increase of burial rate of organic materials and a decrease of the oxygen consumption in sedimentary rocks caused the oxygen content in the air to rise (Des Marais et al., 1992; Karhu and Holland, 1996), the oxidation of Fe^{2+} to Fe^{3+} in seawater and the deposition of BIF (Cloud, 1972). This paper presents a new idea of oxidation of the mantle by a phase change of subducted oceanic crust to Pv-bearing materials at slab penetration. The process decreases the iron content in the upper mantle by the reaction of ferrous to ferric and metallic iron, as shown above. As a result, the reaction increases the $Fe^{3+}/\sum Fe$ ratio of the silicate mantle, concomitant with the growth of a metallic core, and implies an increase of the oxygen fugacity of the mantle through geological time. However, verification is required to analyze the primary $Fe^{3+}/\sum Fe$ ratio of ancient MORB.

The influence of oxidation of the mantle on the surface environment is still poorly understood. Although still controversial (Ohmoto, 1997; Holland, 1999), it is commonly considered that seawater and the atmosphere were reduced before the late Archean, and were suddenly oxidized in the early Proterozoic (e.g., Cloud, 1972; Kasting, 1993; Holland, 1994; Farquhar et al., 2000). Holland (1994) compiled geological evidence for a sudden increase of atmospheric oxygen in the early

Proterozoic: composition of paleosols, initiation of deposition of red shales, existence of manganese deposits, and termination of deposition of BIF and pyrite- and uraninite-rich sedimentary rocks. Kasting (1993) also collected evidence to constrain the upper and lower bounds of the atmospheric oxygen content, and showed its secular change through time. It is also commonly considered that the redox condition of seawater changed from anoxic in the Archean through euxinic in the early to middle Proterozoic to oxic since the Neoproterozoic due to oxidation by the atmosphere, based on geochemical evidence (Arnold et al., 2004; Kah et al., 2004; Poulton et al., 2004; Rouxel et al., 2005) and schematic views (Kasting, 1993; Anbar and Knoll, 2002). Recently, we made in-situ analyses of major, trace and REE of carbonate minerals with primary sedimentary and precipitation structures in sedimentary carbonate rocks and filled-in amygdules and matrices of pillow lavas to estimate the secular change of the redox condition of seawater (Komiya, 2005). The in-situ analyses eliminate secondary carbonate, contamination of detrital materials, diagenesis and alteration. We estimated the depositional environments from the field occurrence of coexisting basaltic lavas and sedimentary rocks and the fabric of the carbonate themselves, and classified them into shallow and deep (>ca. 1000 m) environmental carbonates. The shallow marine deposits include sedimentary carbonates with stromatolite structure and intercalation with clastic beds, and amygdaloidal carbonates of hot-spot basaltic lava since 3.5 Ga. The deep-sea carbonates comprise those in amygdules and matrices of pillow lavas of MORB-type basalts. Deep-sea carbonates have only faint Ce and Eu anomalies between 3.5 and 1.9 Ga. A negative Ce anomaly of shallow carbonates frequently deviated from that of deep-sea carbonate after 2.78 Ga. The anomaly fluctuated considerably, and was very large at 2.5 and 2.3 Ga. But, the anomaly decreased during/after the Huronian and Marinoan, and probably Sturtian glaciations. This implies a complicated secular change of the redox state in shallow water, whereas the deep-sea environment was anoxic until the Proterozoic. We calculated the oxygen content of shallow and deep seawater based on the Ce concentration and anomaly of carbonate minerals at given parameters of atmospheric pCO_2, and Ca^{2+} of seawater. The Ce concentration of seawater was calculated based on a solid solution model of REE in carbonate and the partition coefficient between carbonate and seawater (Tanaka et al., 2004). The Ce anomaly is dependent on the redox potential and pH of seawater as well as the Ce concentration (Akagi and Masuda, 1998). The variation and distribution of REE complexes in seawater also depends on the pH. We calculated the pH of seawater assuming the evolution curves of atmospheric pCO_2 in the Precambrian (Sleep and Zahnle, 2001) and the Phanerozoic (Royer et al., 2004), and assuming $[Ca^{2+}]_{SW}$ at 3.5 Ga (Foriel et al., 2004) and since the Mesozoic (Demicco et al., 2003), and we estimated a pH of 6.39 at 3.5 Ga to 8.3 at present. We calculated redox potentials from the Ce anomaly and concentration, pCO_2 and pH (Akagi and Masuda, 1998). Assuming that the standard potential is 0.84 (Liu et al., 1988), we estimated the dissolved oxygen content of seawater from the reaction of $2H_2O = O_2 + 4H^+ + 4e^-$. The results are shown in Figure 18, and indicate that oxygen activity of deep-sea water was low and constant until at least 1.9 Ga, probably the Mesozoic, whereas that of shallow seawater increased since

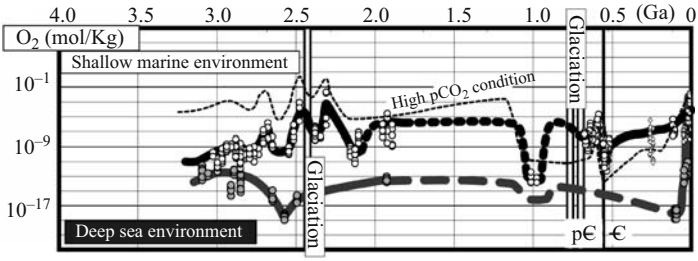


Figure 18. Secular variation of the oxygen contents of shallow marine and deep seawater, respectively. Open circles: carbonate minerals in shallow environment; solid gray circles: deep environment; open diamonds: estimate from composition of Mesozoic carbonate rocks (Tanaka et al., 2003); and open squares: calculated values from modern seawater. Calculations are from Ce anomaly of carbonate minerals through time, secular change of atmospheric CO_2 content (Sleep and Zahnle, 2001 for Precambrian ages; Royer et al., 2004 for Phanerozoic ages), and $[Ca^{2+}]_{SW}$ (Foriel et al., 2004 for 3.5 Ga seawater; Demicco et al., 2003 for the Phanerozoic). Solid solution model of REE in carbonate, and partition coefficient of REE between carbonate and seawater are referred to Tanaka et al. (2004). Standard potential of decomposition of water is 0.84 V (Liu et al., 1988). Temperatures of shallow and deep seawater are assumed to be 15° and 0°C, respectively. A thin dotted line is the oxygen concentration of seawater calculated using a parameter of high atmospheric CO_2, namely average value of a range of atmospheric CO_2 proposed by Kasting (1993). The results show that the oxygen content of deep-sea water was low and constant until at least 1.9 Ga, probably the Mesozoic, whereas that of shallow seawater increased after 2.7 Ga but fluctuated highly. In particular, it reached minima during/after the Snowball Earth events. The oxygen activity became quite high at 2.5 and 2.3 Ga, but it gradually increased in the Phanerozoic.

2.7 Ga but was fluctuated highly. The oxygen activity became quite high at 2.5 and 2.3 Ga, but it eventually increased in the Phanerozoic. Especially, it reached minima during/after Snowball Earth events. However, there are some periods of minima of oxygen content of seawaters, unrelated to Snowball Earth events. Although the causes of them are still unknown, the low oxygen content of seawater around 1.0 Ga probably corresponds to a hiatus in the presence of macrofossils (Hofmann and Chen, 1981; Hofmann and Bengtson, 1992; Hofmann, 1994; Walter et al., 1990; Han and Runnegar, 1992; Kumar, 1995; Zhu and Chen, 1995). High atmospheric CO_2 concentration also explains the small negative Ce anomaly around 1.0 Ga (Fig. 18). Assuming high atmospheric CO_2 concentration through time, namely average value of the estimate by Kasting (1993), we also calculated the dissolved oxygen content of seawater (Fig. 18). The estimate shows the calculated oxygen content of seawater in the Archean was higher than at present, and contradicts many geological observations (Holland, 1994). Therefore, our calculation of dissolved oxygen content of seawater through time favors a low atmospheric CO_2 content through time (e.g., Rye et al., 1995, Sleep and Zahnle, 2001).

BIFs were prominent from 3.8 to 1.8 Ga (Klein et al., 1992). Although there is evidence of oxygenic photosynthetic bacteria, microfossils (e.g., Schopf, 1993) and stromatolites (e.g., Hofmann et al., 1999; Lindsay et al., 2005) only since 3.5 Ga, BIF having been deposited at least since 3.8 Ga. This geological observation is

inconsistent with anoxic seawater in the early Archean. Their formation in an anoxic environment was variably explained by: photochemical reaction (Cairns-Smith, 1978; Braterman et al., 1983; François, 1986; Canuto, 1994), abiotic oxygenic photodissolution (Towe, 1978; Canuto et al., 1982), anaerobic biooxidation of Fe^{2+} (Widdel et al., 1993; Ehrenreich and Widdel, 1994; Hafenbradl et al., 1996; Chaudhuri et al., 2001) and reduction by Fe^{2+} of nitrites and nitrates to prebiotic ammonia (Summers and Chang, 1993; Summers and Lerner, 1998). However, these models are not necessarily consistent with the geological and biological evidence. For example, there is no evidence for such life in the Isua supracrustal belt. High atmospheric pCO_2 resulted in a low pH of the whole seawater, unsuitable for formation of Fe^{3+} as a bi-product of ammonia, whereas the photochemical reaction for Fe^{3+} formation requires quite low pH. BIFs were mostly composed of hematite and iron hydroxide after the middle Archean, whereas BIF in the Isua supracrustal belt mainly contain magnetite. The difference of mineral assemblage is explained by later metamorphism, because hematite is transformed into magnetite at medium-grade metamorphism (Klein, 1983; Dymek and Klein, 1988). However, the mineralogical difference implies a difference of origin. Although generally speaking, hydrothermal fluids have a low pH of 2–6 (Von Damm, 1995), a hydrothermal fluid with a high pH of up to 12 is formed by serpentinization of ultramafic rocks (e.g., Kelley et al., 2005).

Mixing a high pH siliceous hydrothermal fluid and a low pH seawater with a high ferrous content possibly led to precipitation of magnetite and chert under an anoxic environment around a mid-ocean ridge. This hypothesis is consistent with the idea that some BIFs have both negative Ce and positive Eu anomalies. The positive Eu anomaly is caused by precipitation from a hydrothermal fluid (Klinkhammer et al., 1994). Although Dymek and Klein (1988) suggested that a negative Ce anomaly was due to oxic seawater even in the early Archean, the origin of a negative anomaly is still ambiguous. Both anomalies favor the involvement of a hydrothermal fluid with a high pH. If magnetite-type BIF were deposited under an anoxic environment, the BIF in the 3.4 Ga Imataca Complex, Venezuela, is the oldest BIF deposited at least locally in an oxic environment, consistent with the emergence of photosynthetic organisms (James, 1983). However, the photosynthetic organisms did not flourish until the late Archean, because stromatolites became ubiquitous after the late Archean. The prosperity of photosynthetic organisms was also probably due to mantle overturn. The formation of large continents through collision or amalgamation of small continents and island arcs in the late Archean influenced the diversity of life.

Paleomagnetic data show that the intensity of geomagnetism increased in the late Archean (Hale, 1987; Yoshihara and Hamano, 2000) and the increase was caused by formation of the inner core (Stevenson et al., 1983). The geomagnetism was possibly activated by a mantle overturn, because the extensive exchange between the upper and lower mantle materials effectively cooled the core. The intense geomagnetism formed the Van Allen belt, and consequently protected primitive life in the surface environment. However, the ozone layer was still immature, because of low oxygen content in the atmosphere (Kasting, 1993). Therefore, photosynthetic life inhabited tens of meters below the surface of the sea (Berkner and Marshall,

1965). The formation of large continents and their subsequent break-up provided a wide shallow water environment in continental shelves, continental rifts, and intra-continental basins. Especially, the formation of continental rifts and intra-continental basins was indebted to superplume activities; upwelling and downwelling of a super-plume, respectively. Combination of the influence by evolution of a solid earth, which includes oxidation of the mantle through time because of the sink of basaltic materials into the lower mantle and catastrophic upwelling of the lower mantle materials, with the evolution and prosperity of life in plume-related shallow water environments resulted in a sudden increase of atmospheric O_2 in the late Archean to early Proterozoic. The catastrophic evolution of the solid earth was probably induced by mantle overturn.

ACKNOWLEDGEMENTS

This work was partly supported by grants from the Ministry of Education, Culture, Sports, Science and Technology, Japan (No. 04302021, 07238105, 16740284) and by a project on Whole Earth Dynamics from the Science and Technology Agency of Japan. We thank Drs. Takafumi Hirata, Tsuyoshi Iizuka and Shuji Rino for the acquisition of analytical data. We are grateful to Prof. Shigenori Maruyama and Kei Hirose for their constructive comments. The works presented here are based on a number of collaborations with my colleagues including Mamoru Hayashi, Tsuyoshi Iizuka and Shuji Rino. We are grateful to Prof. Brian Windley for his fruitful comments and reviews.

REFERENCES

Abbott, D., L. Burgess, and J. Longhi (1994) An empirical thermal history of the Earth's upper mantle. *J. Geophys. Res.*, 99, 13835–13850.

Akagi, T., and A. Masuda (1998) A simple thermodynamic interpretation of Ce anomaly. *Geochem. J.*, 32, 301–314.

Allègre, C.J. (1982) Chemical geodynamics. *Tectonophysics*, 81, 109–132.

Allègre, C.J., O. Brévart, B. Dupré, and J.-F. Minster (1980) Isotopic and chemical effects produced in a continuously differentiating convecting Earth mantle. *Philos. Trans. R. Soc. Lond. A*, 297, 447–477.

Anbar, A.D., and A.H. Knoll (2002) Proterozoic ocean chemistry and evolution: A bioinorganic bridge? *Science*, 297, 1137–1142.

Arculus, R.J. (1985) Oxidation status of the mantle past and present. *Ann. Rev. Earth Planet. Sci.*, 13, 75–95.

Arculus, R.J., and J.W. Delano (1987) Oxidation state of the upper mantle: Present conditions, evolution, and controls. In Nixon, P.H. (ed.) Mantle Xenoliths, Wiley, New York, pp. 589–599.

Armstrong, R.L. (1981) Radiogenic isotopes: The case for crustal recycling on a near-steady state no-continental-growth Earth. *Philos. Trans. R. Soc. Lond. A*, 301, 443–472.

Arndt, N.T. (1983) Role of a thin, komatiite-rich oceanic crust in the Archean plate-tectonics process. *Geology*, 11, 372–375.

Arndt, N.T. (1991) High Ni in Archean tholeiites. *Tectonophysics*, 187, 411–419.

Arndt, N.T., and E.G. Nisbet (1982) Komatiites, George Allen & Unwin, London, p. 526.

Arnold, G.L., A.D. Anbar, J. Barling, and T.W. Lyons (2004) Molybdenum isotope evidence for widespread anoxia in Mid-Proterozoic oceans. *Science*, 304, 87–90.

Ballhaus, C. (1995) Is the upper mantle metal-saturated? *Earth Planet. Sci. Lett.*, 132, 75–86.
Barley, M.E., and D.I. Groves (1992) Supercontinent cycles and the distribution of metal deposits through time. *Geology*, 20, 291–294.
Bennett, V.C., A.P. Nutman, and M.T. McCulloch (1993) Nd isotopic evidence for transient, highly depleted mantle reservoirs in the early history of the Earth. *Earth Planet. Sci. Lett.*, 119, 299–317.
Berkner, L.V., and L.C. Marshall (1965) On the origin and rise of oxygen concentration in the Earth's atmosphere. *J. Atmospheric Sci.*, 22, 225–261.
Bickle, M.J. (1978) Heat loss from the Earth: A constraint on Archaean tectonics from the relation between geothermal gradients and the rate of plate production. *Earth Planet. Sci. Lett.*, 40, 301–315.
Bickle, M.J., E.G. Nisbet, and A. Martin (1994) Archean greenstone belts are not oceanic crust. *J. Geol.*, 102, 121–138.
Birch, F. (1958) Differentiation of the Mantle. *Geol. Soc. Am. Bull.*, 69, 483–485.
Bleeker, W. (2003) The late Archean record: A puzzle in ca. 35 pieces. *Lithos*, 71, 99–134.
Bowring, S.A., and I.S. Williams (1999) Priscoan (4.00–4.03 Ga) orthogneisses from northwestern Canada. *Contrib. Mineral. Petrol.*, 134, 3–16.
Braterman, P.S., A.G. Cairns-Smith, and R.W. Stolper (1983) Photo-oxidation of hydrated Fe^{2+}-significance for banded iron formations. *Nature*, 303, 163–164.
Breuer, D., and T. Spohn (1995) Possible flush instability in mantle convection at the Archaean-Proterozoic transition. *Nature*, 378, 608–610.
Bridgwater, D., V.R. McGregor, and J.S. Myers (1974) A horizontal tectonic regime in the Archean of Greenland and its implications for early crustal thickening. *Precambrian Res.*, 1, 179–197.
Brown, G.C. (1979) The changing pattern of batholith emplacement during earth history. In Atherton, M.P., and J. Tarney (eds.) Origin of Granite Batholiths, Shiva, Nantwich, UK, pp. 106–115.
Buck, W.R. (1992) Global decoupling of crust and mantle: Implications for topography, geoid and mantle viscosity of venus. *Geophys. Res. Lett.*, 19, 2111–2114.
Burke, K., J.F. Dewey, and W.S.F. Kidd (1976) Dominance of horizontal movements, arc and microcontinental collisions during the later permobile regime. In Windley, B.F. (ed.) The Early History of the Earth, John Wiley & Sons, London, pp. 113–129.
Burke, K., and W.S.F. Kidd (1978) Were Archean continental geothermal gradients much steeper than those of today? *Nature*, 272, 240–241.
Cairns-Smith, A.G. (1978) Precambrian solution photochemistry, inverse segregation, and banded iron formations. *Nature*, 276, 807–808.
Calvert, A.J., E.W. Sawyer, W.J. Davis, and J.N. Ludden (1995) Archaean subduction inferred from seismic images of a mantle suture in the Superior Province. *Nature*, 375, 670–674.
Campbell, I.H., R.W. Griffiths, and R.I. Hill (1989) Melting in an Archaean mantle plume: Heads it's basalts, tails it's komatiites. *Nature*, 339, 697–699.
Canil, D. (1997) Vanadium partitioning and the oxidation state of Archaean komatiite magmas. *Nature*, 389, 842–845.
Canuto, V.M. (1994) Genesis of banded iron-formation. *Economic Geology*, 89, 1384–1397.
Canuto, V.M., J.S. Levine, T.R. Augustsson, and C.L. Imhoff (1982) UV radiation from the young Sun and oxygen and ozone levels in the prebiological palaeoatmosphere. *Nature*, 296, 816–820.
Carmichael, I.S.E. (1991) The redox states of basic and silicic magmas: A reflection of their source regions? *Contrib. Mineral. Petrol.*, 106, 129–141.
Cavosie, A.J., J.W. Valley, S.A. Wilde, and E.I.M.F. (2005) Magmatic $\delta^{18}O$ in 4400–3900 Ma detrital zircons: A record of the alteration and recycling of crust in the Early Archean. *Earth Planet. Sci. Lett.*, 235, 663–681.
Chase, C.G., and P.J. Patchett (1988) Stored mafic/ultramafic crust and early Archean mantle depletion. *Earth Planet. Sci. Lett.*, 91, 66–72.
Chaudhuri, S.K., J.G. Lack, and J.D. Coates (2001) Biogenic Magnetite Formation through Anaerobic Biooxidation of Fe(II). *Appl. Environ. Microbiol.*, 67, 2844–2848.
Chinner, G.A. (1960) Pelitic gneisses with varying ferrous/ferric ratios from Glen Clova, Angus, Scotland. *J. Petrol.*, 1, 178–217.

Christie, D.M., I.S.E. Carmichael, and C.H. Langmuir (1986) Oxidation states of mid-ocean ridge basalt glasses. *Earth Planet. Sci. Lett.*, 79, 397–411.
Cloud, P. (1972) A working model of the primitive Earth. *Am. J. Sci.*, 272, 537–548.
Cohen, R.S., N.M. Evensen, P.J. Hamilton, and R.K. O'Nions (1980) U-Pb, Sm-Nd and Rb-Sr systematics of mid-ocean ridge basalt glasses. *Nature*, 283, 149–153.
Condie, K. (1982) Plate Tectonics and Crustal Evolution, New York, Pergamon, 310p.
Condie, K.C. (1972) A plate tectonics evolutionary model of the South Pass Archaean greenstone belt, southwestern Wyoming. Proc. 24th Int. Geol. Congr., 1, 104–112.
Condie, K.C. (1995) Episodic ages of greenstones: A key to mantle dynamics? *Geophys. Res. Lett.*, 22, 2215–2218.
Condie, K.C. (1998) Episodic continental growth and supercontinents: A mantle avalanche connection? *Earth Planet. Sci. Lett.*, 163, 97–108.
Condie, K.C. (2000) Episodic continental growth models: Afterthoughts and extensions. *Tectonophysics*, 322, 153–162.
Cordani, U.G., K. Sato, W. Teixeira, C.C.G. Tassinari, and M.A.S. Basei (2000) Crustal evolution of the South American platform. In Cordani, U.G., E.J. Milani, A. Thomaz Filho, and D.A. Campos (eds.) Tectonic Evolution of South America, Rio de Janeiro, 31st Inter. Geol. Congr., pp. 19–40.
Cowan, D.S. (1985) Structural styles in Mesozoic and Cenozoic mélanges in the western Cordillera of North America. *Geol. Soc. Am. Bull.*, 96, 451–462.
Davies, G.F. (1980) Thermal histories of convective earth models and constraints on radiogenic heat production in the earth. *J. Geophys. Res.*, 85, 2517–2530.
Davies, G.F. (1992) On the emergence of plate tectonics. *Geology*, 20, 963–966.
Davies, G.F. (1995) Punctuated tectonic evolution of the earth. *Earth Planet. Sci. Lett.*, 136, 363–379.
de Wit, M.J., and R.A. Hart (1993) Earth's earliest continental lithosphere, hydrothermal flux and crustal recycling. *Lithos*, 30, 309–335.
Defant, M.J., and M.S. Drummond (1990) Dehydration of some modern arc magmas by melting of young subducted lithosphere. *Nature*, 347, 662–665.
Delano, J.W. (2001) Redox history of the earth's interior since ~3900 Ma: Implications for prebiotic molecules. *Orig. Life Evol. Biosph.*, 31, 311–341.
Demicco, R.V., T.K. Lowenstein, and L.A. Hardie (2003) Atmospheric pCO2 since 60 Ma from records of seawater pH, calcium, and primary carbonate mineralogy. *Geology*, 31, 793–796.
Des Marais, D.J., H. Strauss, R.E. Summons, and J.M. Hayes (1992) Carbon isotope evidence for the stepwise oxidation of the Proterozoic environment. *Nature*, 359, 605–609.
Dewey, J., and H. Spall (1975) Pre-Mesozoic plate tectonics: How far back in Earth history can the Wilson Cycle be extended? *Geology*, 3, 422–424.
Dewey, J.F., and B.F. Windley (1981) Growth and differentiation of continental crust. *Philos. Trans. R. Soc. Lond. A*, 301, 189–206.
Dupré, B., and C.J. Allègre (1980) Pb-Sr-Nd isotopic correlations and the chemistry of the North Atlantic mantle. *Nature*, 286, 17–22.
Dymek, R.F., and C. Klein (1988) Chemistry, petrology and origin of banded iron-formation lithologies from the 3800 Ma Isua supracrustal belt, West Greenland. *Precambrian Res.*, 39, 247–302.
Eggler, D.H., and J.P. Lorand (1994) Sulfides, diamonds and mantle fO_2. Proc. 5th Int. Kimb. Conf., CPRM Brasilia, Brasilia, pp. 160–169.
Ehrenreich, A., and F. Widdel (1994) Anaerobic oxidation of ferrous iron by purple bacteria, a new type of phototrophic metabolism. *Appl. Environ. Microbiol.*, 60, 4517–4526.
Engebretson, D.C., K.P. Kelley, H.J. Cashman, and M.A. Richards (1992) 180 million years of subduction. *GSA Today*, 2, 93–95, 100.
England, P., and M. Bickle (1984) Continental thermal and tectonic regimes during the Archean. *J. Geol.*, 92, 353–367.
Ernst, R.E., and K.L. Buchan (2002a) Erratum to "Maximum size and distribution in time and space of mantle plumes: Evidence from large igneous provinces". *J. Geodynamics*, 34, 711–714.

Ernst, R.E., and K.L. Buchan (2002b) Maximum size and distribution in time and space of mantle plumes: Evidence from large igneous provinces. *J. Geodynamics*, 34, 309–342.

Farquhar, J., H. Bao, and M. Thiemens (2000) Atmospheric influence of earth's earliest sulfur cycle. *Science*, 289, 756–758.

Foriel, J., P. Philippot, P. Rey, A. Somogyi, D. Banks, and B. Ménez (2004) Biological control of Cl/Br and low sulfate concentration in a 3.5-Gyr-old seawater from North Pole, Western Australia. *Earth Planet. Sci. Lett.*, 228, 451–463.

Fowler, C.M.R., C. Ebinger, and C.J. Hawkesworth (eds) (2002) The early Earth: Physical, chemical and biological development. *Geol. Soc. Lond. Spec. Publ.*, 199, p. 352.

François, L.M. (1986) Extensive deposition of banded iron formations was possible without photosynthesis. *Nature*, 320, 352–354.

Frost, C.D. (1993) Nd isotopic evidence for the antiquity of the Wyoming province. *Geology*, 21, 351–354.

Frost, C.D., B.R. Frost, K.R. Chamberlain, and T.P. Hulsebosch (1998) The Late Archean history of the Wyoming province as recorded by granitic magmatism in the Wind River Range, Wyoming. *Precambrian Res.*, 89, 145–173.

Frost, D.J., C. Liebske, F. Langenhorst, C.A. McCammon, R.G. Trønnes, and D.C. Rubie (2004) Experimental evidence for the existence of iron-rich metal in the Earth's lower mantle. *Nature*, 428, 409–412.

Fukao, Y., M. Obayashi, H. Inoue, and M. Nenbai (1992) Subducting slabs stagnant in the mantle transition zone. *J. Geophys. Res.*, 97, 4809–4822.

Fyfe, W.S. (1978) The evolution of the Earth's crust: Modern plate tectonics to ancient hot spot tectonics. *Chem. Geol.*, 23, 89–114.

Galer, S.J.G., and S.L. Goldstein (1991) Early mantle differentiation and its thermal consequences. *Geochim. Cosmochim. Acta*, 55, 227–239.

Gastil, R.G. (1960) Distribution of mineral dates in time and space. *Am. J. Sci.*, 258, 1–35.

Gladczenko, T.P., M.F. Coffin, and O. Eldholm (1997) Crustal structure of the Ontong Java Plateau: Modeling of new gravity and existing seismic data. *J. Geophys. Res.*, 102, 22711–22729.

Grambling, J.A. (1981) Pressures and temperatures in Precambrian metamorphic rocks. *Earth Planet. Sci. Lett.*, 53, 63–68.

Green, D.H., I.A. Nicholls, M. Viljoen, and R. Viljoen (1975) Experimental demonstration of the existence of peridotitic liquids in earliest Archean magmatism. *Geology*, 3, 11–14.

Gurnis, M., and G.F. Davies (1986) Apparent episodic crustal growth arising from a smoothly evolving mantle. *Geology*, 14, 396–399.

Hafenbradl, D., M. Keller, R. Dirmeier, R. Rachel, P. Ro√ünagel, S. Burggraf, H. Huber, and K.O. Stetter (1996) *Ferroglobus placidus* gen. nov., sp. nov., a novel hyperthermophilic archaeum that oxidizes Fe^{2+} at neutral pH under anoxic conditions. *Arch. Microbiol.*, 166, 308–314.

Hale, C.J. (1987) Palaeomagnetic data suggest link between the Archaean-Proterozoic boundary and inner-core nucleation. *Nature*, 329, 233–237.

Hamilton, W.B. (2003) An alternative Earth. *GSA Today*, pp. 4–12.

Han, T.-M., and B. Runnegar (1992) Megascopic eukaryotic algae from the 2.1 billion-year-old Negaunee Iron-Formation, Michigan. *Science*, 257, 232–235.

Hargraves, R.B. (1986) Faster spreading or greater ridge length in the Archean? *Geology*, 14, 750–752.

Hart, S.R., C. Brooks, T.E. Krogh, G.L. Davis, and D. Nava, 1970, Ancient and modern volcanic rocks: A trace element model. *Earth Planet. Sci. Lett.*, 10, 17–28.

Hauri, E.H., N. Shimizu, J.J. Dieu, and S.R. Hart (1993) Evidence for hotspot-related carbonatite metasomatism in the oceanic upper mantle. *Nature*, 365, 221–227.

Hayashi, M., T. Komiya, Y. Nakamura, and S. Maruyama (2000) Archean regional metamorphism of the Isua supracrustal belt, southern West Greenland: Implications for a driving force of Archean plate tectonics. *Int. Geo. Rev.*, 42, 1055–1115.

Head, J.W., and L.S. Crumpler (1990) Venus geology and tectonics: Hotspot and crustal spreading models and questions for the Magellan mission. *Nature*, 346, 525–533.

Herzberg, C., and J. Zhang (1996) Melting experiments on anhydrous peridotite KLB-1: Compositions of magmas in the upper mantle and transition zone. *J. Geophys. Res.*, 101, 8271–8295.

Hirose, K. (2002) Phase transitions in pyrolitic mantle around 670-km depth: Implications for upwelling of plumes from the lower mantle. *J. Geophys. Res.*, 107, doi: 10.1029/2001JB000597.

Hirose, K., Y. Fei, Y. Ma, and H. Mao (1999) The fate of subducted basaltic crust in the Earth's lower mantle. *Nature*, 397, 53–56.

Hirose, K., N. Shimizu, W. van Westrenen, and Y. Fei (2004) Trace element partitioning in Earth's lower mantle and implications for geochemical consequences of partial melting at the core-mantle boundary. *Phys. Earth Planet. Inter.*, 146, 249–260.

Hoffman, P.F. (1991) On accretion of granite-greenstone terranes. In Robert, F., P.A. Sheahan, and S.B. Green (eds.) Greenstone Gold and Crustal Evolution, Geological Association of Canada, St. John's, Newfoundland, pp. 32–45.

Hoffman, P.F., and G. Ranalli (1988) Archean oceanic flake tectonics. *Geophys. Res. Lett.*, 15, 1077–1080.

Hofmann, A.W., K.P. Jochum, M. Seufert, and W.M. White (1986) Nb and Pb in oceanic basalts: New constraints on mantle evolution. *Earth Planet. Sci. Lett.*, 79, 33–45.

Hofmann, H., and J. Chen (1981) Carbonaceous megafossils from the Precambrian (1800 Ma) near Jixian, northern China. *Can. J. Earth Sci.*, 18, 443–447.

Hofmann, H.J., and S. Bengtson (1992) Stratigraphic distribution of megafossils. In Schopf, J.W., and C. Klein (eds.) The Proterozoic Biosphere, Cambridge University Press, New York, pp. 501–506.

Hofmann, H. (1994) Proterozoic carbonaceous compressions ("metaphytes" and "worms"). In Bengtson, S. (ed.) Early Life on Earth, Columbia University Press, New York, pp. 342–357.

Hofmann, H.J., K. Grey, A.H. Hickman, and R.I. Thorpe (1999) Origins of 3.45 Ga coniform stromatolites in Warrawoona Group, Western Australia. *Geol. Soc. Am. Bull.*, 111, 1256–1262.

Holland, H.D. (1994) Early Proterozoic atmospheric change. In Bengtson, S. (ed.) Early Life on Earth, Columbia University Press, New York, pp. 237–244.

Holland, H.D. (1999) When did the Earth's atmosphere become oxic? *A Reply. The Geochemical News*, 100, 20–22.

Honda, S. (1995) A simple parameterized model of Earth's thermal history with the transition from layered to whole mantle convection. *Earth Planet. Sci. Lett.*, 131, 357–369.

Humayun, M., L. Qin, and M.D. Norman (2004) Geochemical evidence for excess iron in the mantle beneath Hawaii. *Science*, 306, 91–94.

Hurley, P.M., and J.R. Rand (1969) Pre-drift continental nuclei. *Science*, 164, 1229–1242.

Iizuka, T., T. Hirata, T. Komiya, S. Rino, I. Katayama, A. Motoki, and S. Maruyama (2005) U-Pb and Lu-Hf isotope systematics of zircons from the Mississippi River sand: Implications for reworking and growth of continental crust. *Geology*, 33, 485–488.

Iizuka, T., K. Horie, T. Komiya, S. Maruyama, T. Hirata, H. Hidaka, and B.F. Windley (2006) Occurrence of a 4.2 Gyr old zircon in the Acasta Gneiss Complex of northwestern Canada: Geology, v. 34, pp. 245–248.

Inoue, T., and H. Sawamoto (1992) High pressure melting of pyrolite under hydrous condition and its geophysical implication: High-pressure Research. Application to Earth and Planetary Sciences, Tokyo and AGU, Washington D.C., Terra, pp. 323–331.

Irifune, T., and A.E. Ringwood (1987) Phase transformations in a harzburgite composition to 26 GPa: Implications for dynamical behaviour of the subducting slab. *Earth Planet Sci. Lett.*, 86, 365–376.

Isozaki, Y., S. Maruyama, and F. Furuoka (1990) Accreted oceanic materials in Japan. *Tectonophysics*, 181, 179–205.

James, H.L. (1983) Distribution of banded iron-formation in space and time. In Trendall, A.F., and R.C. Morris (eds.) Iron-Formation: Facts and Problems: Developments in Precambrian Geology, Elsevier, Amsterdam, pp. 471–490.

Kah, L.C., T.W. Lyons, and T.D. Frank (2004) Low marine sulphate and protracted oxygenation of the Proterozoic biosphere. *Nature*, 431, 834–838.

Kamber, B.S., K.D. Collerson, S. Moorbath, and M.J. Whitehouse (2003) Inheritance of early Archaean Pb-isotope variability from long-lived Hadean protocrust. *Contrib. Mineral. Petrol.*, 145, 25–46.

Kaminsky, F., O. Zakharchenko, R. Davies, W. Griffin, G. Khachatryan-Blinova, and A. Shiryaev (2001) Superdeep diamonds from the Juina area, Mato Grosso State, Brazil. *Contrib. Mineral. Petrol.*, 140, 734–753.

Karhu, J.A., and H.D. Holland (1996) Carbon isotopes and the rise of atmospheric oxygen. *Geology*, 24, 867–870.

Kasting, J.F. (1993) Earth's early atmosphere. *Science*, 259, 920–926.

Kasting, J.F., D.H. Eggler, and S.P. Raeburn (1993) Mantle redox evolution and the oxidation state of the Archean atmosphere. *J. Geol.*, 101, 245–257.

Kelley, D.S., J.A. Karson, G.L. Fruh-Green, D.R. Yoerger, T.M. Shank, D.A. Butterfield, J.M. Hayes, M.O. Schrenk, E.J. Olson, G. Proskurowski, M. Jakuba, A. Bradley, B. Larson, K. Ludwig, D. Glickson, K. Buckman, A.S. Bradley, W.J. Brazelton, K. Roe, M.J. Elend, A. Delacour, S.M. Bernasconi, M.D. Lilley, J.A. Baross, R.E. Summons, and S.P. Sylva (2005) A serpentinite-hosted ecosystem: The Lost City hydrothermal field. *Science*, 307, 1428–1434.

Kellogg, L.H., B.H. Hager, and R.D. van der Hilst (1999) Compositional stratification in the deep mantle. *Science*, 283, 1881–1884.

Kinny, P.D., W. Compston, and I.A. Williams (1991) A reconnaissance ion-probe study of hafnium isotopes in zircons. *Geochim. Cosmochim. Acta*, 55, 849–859.

Klein, C. (1983) Diagenesis and metamorphism of Precambrian banded iron-formations. In Trendall, A.F., and R.C. Morris (eds.) Iron-Formation: Facts and Problems: Developments in Precambrian Geology, Elsevier, Amsterdam, pp. 417–469.

Klein, C., N.J. Beukes, H.D. Holland, J.F. Kasting, L.R. Kump, and D.R. Lowe (1992) 4. Proterozoic Atmosphere and Ocean. In Schopf, J.W., and C. Klein (eds.) The Proterozoic Biosphere: A Multidisciplinary Study, Cambridge University Press, New York, pp. 135–174.

Klinkhammer, G., C.R. German, H. Elderfield, M.J. Greaves, and A. Mitra (1994) Rare earth elements in hydrothermal fluids and plume particulates by inductively coupled plasma mass spectrometry. *Mar. Chem.*, 45, 179–186.

Komiya, T., S. Maruyama, S. Nohda, T. Masuda, M. Hayashi, and S. Okamoto (1999) Plate tectonics at 3.8–3.7 Ga: Field evidence from the Isua accretionary complex, southern West Greenland. *J Geol.*, 107, 515–554.

Komiya, T., M. Hayashi, S. Maruyama, and H. Yurimoto (2002a) Intermediate-P/T type Archean metamorphism of the Isua supracrustal belt: Implications for secular change of geothermal gradients at subduction zones and for Archean plate tectonics. *Am. J. Sci.*, 302, 804–826.

Komiya, T., T. Iizuka, I. Katayama, Y. Ueno, and Y. Uehara (2002b) Geology of the Acasta Gneiss Complex in Slave Province, northern Canada: Appreciating new geological evidence of the oldest rocks in the world: EOS Trans. AGU, 83(47), Fall Meet. Suppl., Abstract, p. V51B-1243.

Komiya, T., S. Maruyama, T. Hirata, and H. Yurimoto (2002c) Petrology and geochemistry of MORB and OIB in the mid-Archean North Pole region, Pilbara craton, Western Australia: Implications for the composition and temperature of the upper mantle at 3.5 Ga. *Int. Geol. Rev.*, 44, 988–1016.

Komiya, T. (2004) Material circulation model including chemical differentiation within the mantle and secular variation of temperature and composition of the mantle. *Phys. Earth Planet. Inter.*, 146, 333–367.

Komiya, T., S. Maruyama, T. Hirata, H. Yurimoto, and S. Nohda (2004) Geochemistry of the oldest MORB and OIB in the Isua supracrustal belt (3.8 Ga), southern West Greenland: Implications for the composition and temperature of early Archean upper mantle. *The Island Arc*, 13, 47–72.

Komiya, T. (2005) Secular variation of REE patterns of carbonate minerals through the time. EOS Trans. AGU, v. 86, p. Fall Meet. Suppl., Abstract.

Kono, Y., and T. Yoshii (1975) Numerical experiments on the thickening plate model. *J. Phys. Earth*, 23, 63–75.

Kröner, A. (1977) The Precambrian geotectonic evolution of Africa: Plate accretion versus plate destruction. *Precambrian Res.*, 4, 163–213.

Kröner, A. (1981) Precambrian Plate Tectonics. In Kröner, A. (ed.) Precambrian Plate Tectonics, Elsevier, Amsterdam, 57–90.

Kumar, S. (1995) Megafossils from the Mesoproterozoic Rohtas Formation (the Vindhyan Supergroup), Katni area, central India. *Precambrian Res.*, 72, 171–184.

Kump, L.R., J.F. Kasting, and M.E. Barley (2001) Rise of atmospheric oxygen and the "upside-down" Archean mantle. *Geochem. Geophys. Geosyst.*, 2, 2000GC000114.

Kusky, T.M. (1989) Accretion of the Archean Slave province. *Geology*, 17, 63–67.

Kusky, T.M., J.-H. Li, and R.D. Tucker (2001) The Archean Dongwanzi ophiolite complex, North China Craton: 2.505-billion-year-old oceanic crust and mantle. *Science*, 292, 1142–1145.

Kusky, T.M., and P.A. Winsky (1995) Structural relationships along a greenstone/shallow water shelf contact, Belingwe greenstone belt, Zimbabwe. *Tectonics*, 14, 448–471.

Larson, R.L., and C. Kincaid (1996) Onset of mid-Cretaceous volcanism by elevation of the 670 km thermal boundary layer. *Geology*, 24, 551–554.

Lindsay, J.F., M.D. Brasier, N. McLoughlin, O.R. Green, M. Fogel, A. Steele, and S.A. Mertzman (2005) The problem of deep carbon—An Archean paradox. *Precambrian Res.*, 143, 1–22.

Liu, Y.-G., M.R.U. Miah, and R.A. Schmitt (1988) Cerium: A chemical tracer for paleo-oceanic redox conditions. *Geochim. Cosmochim. Acta*, 52, 1361–1371.

Lécuyer, C., and Y. Ricard (1999) Long-term fluxes and budget of ferric iron: Implication for the redox states of the Earth's mantle and atmosphere. *Earth Planet. Sci. Lett.*, 165, 197–211.

Maas, R., P.D. Kinny, I.S. Williams, D.O. Froude, and W. Compston (1992) The Earth's oldest known crust: A geochronological and geochemical study of 3900–4200 Ma old detrital zircons from Mt. Narryer and Jack Hills, Western Australia. *Geochim. Cosmochim. Acta*, 56, 1281–1300.

Martin, H. (1986) Effect of steeper Archean geothermal gradient on geochemistry of subduction-zone magmas. *Geology*, 14, 753–756.

Maruyama, S. (1994) Plume tectonics. *Jour. Geol. Soc. Jpn.*, 100, 24–49.

Maruyama, S., Masuda, S. and Appel, P.W.U. (1991a) The oldest accretionary complex on the Earth, Isua, Greenland. *Geol. Soc. Am., Abstract with programs*, 23, A429-A430.

Maruyama, S., Y. Isozaki, and G. Kimura (1991b) Is the Mid-Archean barite formation from the Pilbara craton, Australia under the deep-sea environment? EOS Trans., 72, p. 532.

Maruyama, S., J.G. Liou, and M. Terabayashi (1996) Blueschists and eclogites of the world and their exhumation. *International Geology Review*, 38, 485–594.

Matsuda, T., and Y. Isozaki (1991) Well-documented travel history of Mesozoic pelagic chert in Japan. *Tectonics*, 10, 475–499.

McCammon, C. (1997) Perovskite as a possible sink for ferric iron in the lower mantle. *Nature*, 387, 694–696.

McCammon, C., M. Hutchison, and J. Harris (1997) Ferric iron content of mineral inclusions in diamonds from São Liz: A view into the lower mantle. *Science*, 278, 434–436.

McCulloch, M.T. (1987) Sm-Nd isotopic constraints on the evolution of Precambrian crust in the Australian continent. In Kröner, A. (ed.) Proterozoic Lithospheric Evolution: Geodynamics, American Geophysical Union, Washington D.C., pp. 115–130.

McCulloch, M.T. (1993) The role of subducted slabs in an evolving earth. *Earth Planet. Sci. Lett.*, 115, 89–100.

McCulloch, M.T., and V.C. Bennett (1994) Progressive growth of the Earth's continental crust and depleted mantle: Geochemical constraints. *Geochim. Cosmochim. Acta*, 58, 4717–4738.

McCulloch, M.T., and G.J. Wasserburg (1979) Sm-Nd and Rb-Sr chronology of continental crust formation. *Science*, 200, 1003–1011.

McDonough, W.F., and S.-S. Sun (1995) The composition of the Earth. *Chem. Geol.*, 120, 223–253.

McGregor, V.R. (1973) The early Precambrian gneisses of the Godthåb district, West Greenland. *Philos. Trans. Royal Soc. Lond. A*, 273, 343–358.

McGregor, V.R. (1993) Descriptive text to 1:100000 Geological map of GREENLAND Qôrqut 64 V.1 Syd.: Copenhagen, Geological Survey of Greenland, 40p.

McGregor, V.R., C.R.L. Friend, and A.P. Nutman (1991) The late Archean mobile belt through Godthåbsfjord, southern West Greenland: A continent-continent collision zone? *Bull. Geol. Soc. Denmark*, 39, 179–197.

McLennan, S.M., and S.R. Taylor (1982) Geochemical constraints on the growth of the continental crust. *J. Geol.*, 90, 342–361.

Miyashiro, A. (1973) Metamorphism and Metamorphic Belts. George Allen & Unwin, London, 492p.

Moorbath, S. (1977) Ages, isotopes and evolution of Precambrian continental crust. *Chem. Geol.*, 20, 151–187.

Moores, E.M. (1993) Neoproterozoic oceanic crustal thinning, emergence of continents and origin of the Phanerozoic ecosystem: A model. *Geology*, 21, 5–8.

Mueller, R.F. (1960) Compositional characteristics and equilibrium relations in mineral assemblages of a metamorphosed iron formation. *Am. J. Sci.*, 258, 449–497.

Nelson, B.K., and D.J. DePaolo (1985) Rapid production of continental crust 1.7 to 1.9 b.y. ago: Nd isotopic evidence from the basement of the North American mid-continent. *Geol. Soc. Am. Bull.*, 96, 746–754.

Nelson, D.R., B.W. Robinson, and J.S. Myers (2000) Complex geological histories extending for $\geq$ 4.0 Ga deciphered from xenocryst zircon microstructures. *Earth Planet. Sci. Lett.*, 181, 89–102.

Newsom, H.E., W.M. White, K.P. Jochum, and A.W. Hofmann (1986) Siderophile and chalcophile element abundances in oceanic basalts, Pb isotope evolution and growth of the Earth's core. *Earth Planet. Sci. Lett.*, 80, 299–313.

Nisbet, E.G., M.J. Cheadle, N.T. Arndt, and M.J. Bickle (1993) Constraining the potential temperature of the Archean mantle: A review of the evidence from komatiites. *Lithos*, 30, 291–307.

Nisbet, E.G., and C.M.R. Fowler (1983) Model for Archean plate tectonics. *Geology*, 11, 376–379.

Nowell, G.M., P.D. Kempton, S.R. Noble, J.G. Fitton, A.D. Saunders, J.J. Mahoney, and R.N. Taylor (1998) High precision Hf isotope measurements of MORB and OIB by thermal ionisation mass spectrometry: Insights into the depleted mantle. *Chem. Geol.*, 149, 211–233.

Nutman, A.P., V.R. McGregor, C.R.L. Friend, V.C. Bennett, and P.D. Kinny (1996) The Itsaq Gneiss Complex of southern West Greenland: The world's most extensive record of early crustal evolution (3,900–3,600 Ma). Precam. Res. Special Issue. *The Oldest Rocks on Earth*, v. 78, pp. 1–39.

O'Neill, H.S.C., D.C. Rubie, D. Canil, C.A. Geiger, C.R. Ross II, F. Seifert, and A.B. Woodland (1993) Ferric iron in the upper mantle and in transition zone assemblages: Implications for relative oxygen fugacities in the mantle. In Takahashi, E., R. Jeanloz, and D. Rubie (eds.) Evolution of the Earth and Planets, IUGG and Am. Geophys. Union, Washington, pp. 73–88.

O'Nions, R.K., N.M. Evensen, and P.J. Hamilton (1979) Geochemical modeling of mantle differentiation and crustal growth. *J. Geophys. Res.*, 84, 6091–6101.

Ogawa, M. (1997) A bifurcation in the coupled magmatism-mantle convection system and its implications for the evolution of the Earth's upper mantle. *Phys. Earth Planet. Inter.*, 102, 259–276.

Ohmoto, H. (1997) When did the Earth's atmosphere become oxic? *Geochem. News*, 93, 12–13, 26–27.

Ohta, H., S. Maruyama, E. Takahashi, Y. Watanabe, and Y. Kato (1996) Field occurrence, geochemistry and petrogenesis of the Archean mid-oceanic ridge basalts (AMORBs) of the Cleaverville area, Pilbara craton, Western Australia. *Lithos*, 37, 199–221.

Okamoto, K., and S. Maruyama (1999) The high-pressure synthesis of lawsonite in the MORB + H_2O system. *Am. Mineral.*, 84, 362–373.

Oldenburg, D.W., and J.N. Brune (1972) Ridge transform fault spreading pattern in freezing wax. *Science*, 178, 301–304.

Parman, S.W., J.C. Dann, T.L. Grove, and M.J. de Wit (1997) Emplacement conditions of komatiite magmas from the 3.49 Ga Komati Formation, Barberton Greenstone Belt, South Africa. *Earth Planet. Sci. Lett.*, 150, 303–323.

Patchett, P.J., J.D. Vervoort, U. Soderlund, and V.J.M. Salters (2004) Lu-Hf and Sm-Nd isotopic systematics in chondrites and their constraints on the Lu-Hf properties of the Earth. *Earth Planet. Sci. Lett.*, 222, 29–41.

Peacock, S.M. (1996) Thermal and petrological structure of subduction zones. In Bebout, G.E., D.W. Scholl, S.H. Kirby, and J.P. Platt (eds.) Subduction: Top to Bottom: Geophys. Monor., Am. Geophys. Union, Washington D.C., pp. 119–133.

Peltier, W.R., S. Butler, and L.P. Solheim (1997) The influence of phase transformations on mantle mixing and plate tectonics. In Crossley, D.J. (ed.) Earth's Deep Interior, Gordon & Breach, Amsterdam, pp. 405–430.

Phillips, R.J., W.M. Kaula, G.E. McGill, and M.C. Malin (1981) Tectonics and evolution of Venus. *Science*, 212, 879–887.

Piper, J.D.A. (1982) The Precambrian palaeomagnetic record: The case for the Proterozoic supercontinent. *Earth Planet. Sci. Lett.*, 59, 61–89.

Pollack, H.N. (1980) The heat flow from the earth: A review. In Davies, P.A., and S.K. Runcorn (eds.) Mechanisms of Continental Drift and Plate Tectonics, Academic Press, New York, pp. 183–192.

Poulton, S.W., P.W. Fralick, and D.E. Canfield (2004) The transition to a sulphidic ocean [sim] 1.84 billion years ago. *Nature*, 431, 173–177.

Rapp, R.P., and E.B. Watson (1995) Dehydration melting of metabasalt at 8–32 kbar: Implications for continental growth and crust-mantle recycling. *J. Petrol.*, 36, 891–931.

Reymer, A., and G. Schubert (1984) Phanerozoic addition rates to the continental crust and crustal growth. *Tectonics*, 3, 63–77.

Richardson, S.H., J.J. Gurney, A.J. Erlank, and J.W. Harris (1984) Origin of diamonds in old enriched mantle. *Nature*, 310, 198–202.

Richter, F.M. (1985) Models for the Archean thermal regime. *Earth Planet. Sci. Lett.*, 73, 350–360.

Righter, K., M.J. Drake, and G. Yaxley (1997) Prediction of siderophile element metal-silicate partition coefficients to 20 GPa and 2800°C: The effects of pressure, temperature, oxygen fugacity, and silicate and metallic melt compositions. *Phys. Earth Planet. Inter.*, 100, 115–134.

Rino, S., T. Komiya, B.F. Windley, I. Katayama, A. Motoki, and T. Hirata (2004) Major episodic increases of continental crustal growth determined from zircon ages of river sands; implications for mantle overturns in the Early Precambrian. *Phys. Earth Planet. Inter.*, 146, 369–394.

Rouxel, O.J., A. Bekker, and K.J. Edwards (2005) Iron isotope constraints on the Archean and Paleoproterozoic ocean redox state. *Science*, 307, 1088–1091.

Royer, D.L., R.A. Berner, I.P. Montañez, N.J. Tabor, and D.J. Beerling (2004) CO2 as a primary driver of Phanerozoic climate. *GSA Today*, 4–10.

Runcorn, S.K. (1965) Changes in the convection pattern in the Earth's mantle and continental drift: Evidence for a cold origin of the Earth. *Philos. Trans. R. Soc. Lond. A*, 258, 228–251.

Rye, R., P.H. Kuo, and H.D. Holland (1995) Atmospheric carbon dioxide concentrations before 2.2 billion years ago. *Nature*, 378, 603–605.

Sakurai, R., T. Komiya, K. Okamoto, K. Shimizu, and K. Hirose (2001) Structural geology and petrology of the Barberton Greenstone Belts, South Africa. 4th International Archean Symposium, pp. 87–89.

Salters, V.J.M., and A. Zindler (1995) Extreme 176Hf/177Hf in the sub-oceanic mantle. *Earth Planet. Sci. Lett.*, 129, 13–30.

Scherer, E., C. Münker, and K. Mezger (2001) Calibration of the Lutetium-Hafnium Clock. *Science*, 293, 683–687.

Schopf, J.W. (1993) Microfossils of the Early Archean Apex Chert: New evidence of the antiquity of life. *Science*, 260, 640–646.

Sclater, J.G., C. Jaupart, and D. Galson (1980) The heat flow through oceanic and continental crust and the heat loss from the earth. *Rev. Geophys. Space Phys.*, 18, 269–311.

Sleep, N.H., and K.J. Zahnle (2001) Carbon dioxide cycling and implications for climate on ancient Earth. *J. Geophys. Res.*, 106, 1373–1399.

Spear, F.S. (1993) Metamorphic Phase Equilibria and Pressure-Temperature-Time Paths, Mineralogical Society of America, Washington, D.C., 799p.

Stachel, T., J.W. Harris, G.P. Brey, and W. Joswig (2000) Kankan diamonds (Guinea) II: Lower mantle inclusion parageneses. *Contrib. Mineral. Petrol.*, 140, 16–27.

Stein, M., and A.W. Hofmann (1994) Mantle plumes and episodic crustal growth. *Nature*, 372, 63–68.
Stern, R.A., E.C. Syme, A.H. Bailes, and S.B. Lucas (1995) Paleoproterozoic (1.90–1.86 Ga) arc volcanism in the Flin Flon Belt, Trans-Hudson Orogen, Canada. *Contrib. Mineral. Petrol.*, 119, 117–141.
Stern, R.J. (2005) Evidence from ophiolites, blueschists, and ultrahigh-pressure metamorphic terranes that the modern episode of subduction tectonics began in Neoproterozoic time. *Geology*, 33, 557–560.
Stevenson, D.J., T. Spohn, and G. Schubert (1983) Magnetism and thermal evolution of terrestrial planets. *Icarus*, 54, 466–489.
Summers, D., and N. Lerner (1998) Ammonia from iron (II) reduction of nitrite and the Strecker synthesis: Do iron (II) and cyanide interfere with each other? *Orig. Life and Evol. Biosph.*, 28, 1–11.
Summers, D.P., and S. Chang (1993) Prebiotic ammonia from reduction of nitrite by iron (II) on the early Earth. *Nature*, 365, 630–633.
Sun, S.-S. (1984) Geochemical characteristics of Archaean ultramafic and mafic volcanic rocks: Implications for mantle composition and evolution. In Kröner, A., G.N. Hansen, and A.M. Goodwin (eds.) Archaean Geochemistry, Springer-Verlag, Berlin, pp. 25–46.
Symmes, G.H., and J.M. Ferry (1992) The effect of whole-rock MnO content on the stability of garnet in pelitic schists during metamorphism. *J. Metamorphic Geol.*, 10, 221–237.
Tajika, E., and T. Matsui (1990) The evolution of the terrestrial environment. In Newsom, H.E., and J.H. Jones (eds.) Origin of the Earth, Oxford University Press, New York, pp. 347–370.
Takahashi, E. (1990) Speculations on the Archean mantle: Missing link between komatiite and depleted garnet peridotite. *J. Geophys. Res.*, 95, 15941–15954.
Takahashi, E., and C.M. Scarfe (1985) Melting of peridotite to 14 GPa and the genesis of komatiites. *Nature*, 315, 566–568.
Tanaka, K., N. Miura, Y. Asahara, and I. Kawabe (2003) Rare earth element and strontium isotopic study of seamount-type limestones in Mesozoic accretionary complex of Southern Chichibu Terrane, central Japan: Implication for incorporation process of seawater REE into limestones. *Geochem. J.*, 37, 163–180.
Tanaka, K., A. Ohta, and I. Kawabe (2004) Experimental REE partitioning between calcite and aqueous solution at 25°C and 1 atm: Constraints on the incorporation of seawater REE into seamount-type limestones. *Geochem. J.*, 38, 19–32.
Taylor, S.R., and S.M. McLennan (1985) The Continental Crust: Its Composition and Evolution, Blackwell, Oxford, 312 p.
Tomlinson, K.Y., G.M. Stott, J.A. Percival, and D. Stone (2004) Basement terrane correlations and crustal recycling in the western Superior Province: Nd isotopic character of granitoid and felsic volcanic rocks in the Wabigoon subprovince, N. Ontario, Canada. *Precambrian Res.*, 132, 245–274.
Towe, K.M. (1978) Early Precambrian oxygen: A case against photosynthesis. *Nature*, 274, 657–661.
Tozer, D.C. (1965) Heat transfer and convection currents. *Philos. Trans. R. Soc. Lond. A*, 258, 252–271.
Turcotte, D.L., and G. Schubert (1982) Geodynamics: Applications of Continuum Physics to Geological Problems, John Wiley & Sons, New York, 450p.
Ueda, H., M. Kawamura, and K. Niida (2000) Accretion and tectonic erosion processes revealed by the mode of occurrence and geochemistry of greenstones in the Cretaceous accretionary complexes of the Idonnappu Zone, southern central Hokkaido, Japan. *The Island Arc*, 9, 237–257.
Urey, H.C. (1956) The cosmic abundance of potassium, uranium, and thorium and the heat balances of the earth, moon, and Mars. *Proc. Natl. Acad. Sci. USA*, 42, 889–891.
Veizer, J., and S.L. Jansen (1979) Basement and sedimentary recycling and continental evolution. *J. Geol.*, 87, 341–370.
Vervoort, J.D., and J. Blichert-Toft (1999) Evolution of the depleted mantle: Hf isotope evidence from juvenile rocks through time. *Geochim. Cosmochim. Acta*, 63, 533–556.
Vielzeuf, D., and M.W. Schmidt (2001) Melting relations in hydrous systems revisited: Application to metapelites, metagreywackes and metabasalts. *Contrib. Mineral. Petrol.*, 141, 251–267.
Von Damm, K.L. (1995) Controls on the chemistry and temporal variability of seafloor hydrothermal fluids. In Humphris, S.E., R.A. Zierenberg, L.S. Mullineaux, and R.E. Thompson (eds.)

Seafloor Hydrothermal Systems: Geophysical Monograph, American Geophysical Union, Washington, pp. 222–247.

Wakita, K., and I. Metcalfe (2005) Ocean Plate Stratigraphy in East and Southeast Asia. *J. Asian Earth Sci.*, 24, 679–702.

Walter, M.R., D. Rulin, and R.J. Horodyski (1990) Coiled carbonaceous megafossils from the Middle Proterozoic of Jixian (Tianjin) and Montana. *Am. J. Sci.*, 290-A, 133–148.

Warren, P.H. (1985) The magma ocean concept and lunar evolution. *Ann. Rev. Earth Planet. Sci.*, 13, 201–240.

Watson, E.B., and T.M. Harrison (2005) Zircon thermometer reveals minimum melting conditions on Earliest Earth. *Science*, 308, 841–844.

Watson, J.V. (1978) Precambrian thermal regimes. *Philos. Trans. R. Soc. Lond. A*, 288, 431–440.

Widdel, F., S. Schunell, S. Heising, A. Ehrenreich, B. Assmus, and B. Schink (1993) Ferrous iron oxidation by anoxygenic phototrophic bacteria. *Nature*, 362, 834–836.

Wilde, S.A., J.W. Valley, W.H. Peck, and C.M. Graham (2001) Evidence from detrital zircons for the existence of continental crust and oceans on the Earth 4.4 Gyr ago. *Nature*, 409, 175–178.

Windley, B.F. (1976) New tectonic models for the evolution of Archean continents and oceans. In Windley, B.F. (ed.) The Early History of the Earth, John Wiley and Sons, London, pp. 105–111.

Windley, B.F. (2003) Continental growth in the Proterozoic: A global perspective. In Yoshida, M., B.F. Windley, and S. Dasgupta (eds.) Proterozoic East Gondwana: Supercontinent Assembly and Breakup, *Geol. Soc. Lond. Spec. Pub.*, pp. 23–33.

Wood, B.J., and D.C. Rubie (1996) The effect of alumina on phase transformations at the 660-kilometer discontinuity from Fe-Mg partitioning experiments. *Science*, 273, 1522–1524.

Wooden, J.L., P.A. Mueller, D.A. Mogk, and D.R. Bowes (1988) A review of the geochemistry and geochronology of Archean rocks of the Beartooth Mountains, Montana and Wyoming: Precambrian and Mesozoic Plate Margins. *Montana Bureau of Mines and Geology Special Publication*, 96, 23–42.

Wynne-Edwards, H.R. (1976) Proterozoic ensialic orogenesis: The millipede model of ductile plate tectonics. *Am. J. Sci.*, 276, 927–953.

Yoshihara, A., and Y. Hamano (2000) Intensity of the Earth's magnetic field in late Archean obtained from diabase dikes of the Slave Province, Canada. *Phys. Earth Planet. Inter.*, 117, 295–307.

Yuen, D.A., D.M. Reuteler, S. Balachandar, V. Steinbach, A.V. Malevsky, and J.J. Smedsmo (1994) Various influences on three-dimensional mantle convection with phase transitions. *Phys. Earth Planet. Inter.*, 86, 185–203.

Zhu, S., and H. Chen (1995) Megascopic multicellular organisms from the 1700-million-year-old Tuanshanzi Formation in the Jixian area, North China. *Science*, 270, 620–622.

Zindler, A., and S. Hart (1986) Chemical geodynamics. *Ann. Rev. Earth Planet. Sci.*, 14, 493–571.